

# Calculation of P-Wave Charmonium Decay Rates Using Dimensional Regularization

Eric Braaten and Yu-Qi Chen

*Physics Department, Ohio State University, Columbus OH 43210*

## Abstract

Contributions to the decay rates of P-wave charmonium states that are proportional to  $n_f \alpha_s^3$ , where  $n_f$  is the number of flavors of light quarks, are calculated in the framework of nonrelativistic QCD using the threshold expansion method. Dimensional regularization is used to regularize the infrared divergences that arise from the emission of a soft gluon. Our results are consistent with the original calculations of Barbieri et al.

## I. INTRODUCTION

The nonrelativistic QCD (NRQCD) factorization formalism [1] provides a systematic framework for analyzing annihilation decay rates and inclusive production rates of heavy quarkonium. These rates are factored into short-distance coefficients and long-distance NRQCD matrix elements. The short-distance coefficients can be calculated using perturbative QCD as a power series in the strong coupling constant  $\alpha_s(m_c)$  at the scale of the heavy quark mass. The matrix elements scale in a definite way with  $v$ , the typical relative velocity of the heavy quark. The NRQCD factorization formalism therefore organizes the decay rate or production rate into a double expansion in powers of  $\alpha_s$  and  $v$ .

The *threshold expansion method* [2] is a general method for calculating the short-distance coefficients which fully exploits the NRQCD factorization formalism. In this method, a quantity that is closely related to the creation or annihilation rate of a  $c\bar{c}$  pair near threshold is calculated using perturbation theory in full QCD and then expanded in powers of the relative 3-momentum  $\mathbf{q}$  of the  $c$  and  $\bar{c}$ . Matrix elements of 4-fermion operators in NRQCD are also calculated using perturbation theory and expanded around the threshold  $\mathbf{q} = 0$ . The short-distance coefficients in the factorization formula are then determined by matching these expansions in  $\mathbf{q}$  order by order in  $\alpha_s$ . Finally, the NRQCD matrix elements for specific quarkonium states are simplified by using rotational symmetry, heavy-quark spin symmetry, and the vacuum-saturation approximation.

In calculating the short-distance coefficients beyond leading order in  $\alpha_s$ , ultraviolet divergences and infrared divergences inevitably arise and need to be regularized. In perturbative calculations, the most convenient method for regularizing both ultraviolet and infrared divergences is dimensional regularization. We recently generalized the threshold expansion method to  $N$  spatial dimensions, so that dimensional regularization can be used consistently in quarkonium calculations [3]. The QCD side of the matching condition and the matrix elements on the NRQCD side are calculated in  $N$  dimensions using perturbation theory and then matched to obtain the short-distance coefficients. After renormalization of

coupling constants in QCD and NRQCD, the short-distance coefficients may have poles in  $N - 3$ , which must be removed by renormalization of the 4-fermion operators in NRQCD. One must take care to avoid simplifying the matrix elements of these operators using identities that are specific to 3 dimensions until after these renormalizations have been carried out. We illustrated our method by calculating gluon fragmentation functions to S-wave and P-wave charmonium states, resolving a discrepancy between two previous calculations of the fragmentation function for  $g \rightarrow \chi_{cJ}$ .

There are also discrepancies in the literature between various calculations of the annihilation decay rates for P-wave states. In the original calculations by Barbieri et al. [4,5], either the binding energy of the  $c\bar{c}$  pair or the energy resolution of a gluon jet was used as the infrared cutoff. In recent calculations by Huang and Chao [6] and by Petrelli [7], dimensional regularization was used for the infrared cutoff. The discrepancies between their results and those of Barbieri et al. appear in the terms proportional to  $n_f\alpha_s^3$ , where  $n_f$  is the number of light quark flavors. This is the term that is sensitive to the infrared cutoff. In this paper, we use the threshold expansion method in conjunction with dimensional regularization to calculate the term proportional to  $n_f\alpha_s^3$ . We find that the discrepancy between the results of Barbieri et al. and the recent calculations using dimensional regularization is due simply to different definitions of a color-octet NRQCD matrix element.

The outline of the rest of this paper is as follows. In Section II, we review the threshold expansion method in  $N$  dimensions as it applies to decay rates. In Section III, we calculate the terms proportional to  $n_f\alpha_s^2$  in the short-distance coefficients of color-octet matrix elements and the terms proportional to  $\alpha_s^2$  and  $n_f\alpha_s^3$  in the short-distance coefficients of color-singlet matrix elements. In Section IV, we apply our results to the decay rates of spin-singlet S-wave and spin-triplet P-wave states. Finally, we compare our results for the P-wave states with the previous calculations in the literature.

## II. THRESHOLD EXPANSION METHOD

The threshold expansion method for calculating the short-distance coefficients in inclusive production cross-sections was developed in Ref. [2] and generalized to  $N$  spatial dimensions in Ref. [3]. In this section, we review this method as it applies to annihilation decay rates, since many of the formulas differ a little from the production case.

The annihilation decay rate for the charmonium state  $H$  can be written in the factorized form [1]

$$\Gamma(H) = \frac{1}{2M_H} \sum_{mn} \frac{C_{mn}(\mu)}{m_c^{d_{mn}-N-1}} \langle H | \mathcal{O}_{mn} | H \rangle^{(\mu)}, \quad (1)$$

where  $M_H$  is the mass of the state  $H$  and  $d_{mn}$  is the mass dimension of the operator  $\mathcal{O}_{mn}$ . The matrix elements  $\langle H | \mathcal{O}_{mn} | H \rangle$  are expectation values in the quarkonium state  $H$  of local 4-fermion operators that have the structure

$$\mathcal{O}_{mn} = \psi^\dagger \mathcal{K}'_m \chi \chi^\dagger \mathcal{K}_n \psi, \quad (2)$$

where  $\psi$  and  $\chi$  are the field operators for the heavy quark and antiquark in NRQCD, and  $\mathcal{K}_n$  and  $\mathcal{K}'_m$  are products of a color matrix (1 or  $T^a$ ), a spin matrix, and a polynomial in the gauge covariant derivative  $\mathbf{D}$  in  $N$  dimensions. The spin matrix is either the unit matrix or a polynomial in the Pauli matrices  $\sigma^i$ . The Pauli matrices in  $N$  dimensions satisfy the anticommutation relations  $\{\sigma_i, \sigma_j\} = 2\delta_{ij}$ ,  $i, j = 1, \dots, N$ . In 3 dimensions, they also satisfy the commutation relations  $[\sigma_i, \sigma_j] = 2i \epsilon_{ijk} \sigma_k$ ,  $i, j, k = 1, 2, 3$ . The commutation relations can be used together with the anticommutation relations to reduce all spin matrices to a linear combination of 1 and  $\sigma^i$ . However, since the commutation relations are specific to  $N = 3$  dimensions, they should be used to simplify NRQCD matrix elements only after all poles in  $N - 3$  have been removed from the short-distance coefficients.

For the purpose of calculating short-distance coefficients, it is convenient to define the states  $|H\rangle = |H(\mathbf{P} = 0)\rangle$  in (1) so that they have the standard relativistic normalization:

$$\langle H(\mathbf{P}') | H(\mathbf{P}) \rangle = 2E_P (2\pi)^N \delta^N(\mathbf{P} - \mathbf{P}'), \quad (3)$$

where  $E_P = \sqrt{M_H^2 + \mathbf{P}^2}$ . With this choice of normalization, the matrix elements in (1) differ from the standard NRQCD matrix elements  $\langle H | \mathcal{O}_1^{(2S+1)L_J} | H \rangle$  and  $\langle H | \mathcal{O}_8^{(2S+1)L_J} | H \rangle$  introduced in Ref. [1]. The relation between them is discussed in Appendix B of [2]. Up to corrections of relative order  $v^2$ , the difference is a simple multiplicative factor. The renormalization of the operators  $\mathcal{O}_{mn}$  makes them depend on the renormalization scale  $\mu$  of NRQCD, as indicated by the superscript  $(\mu)$  on the matrix elements in (1). This dependence will be suppressed whenever it is not essential.

The factors of  $m_c$  in (1) are chosen so that the short-distance coefficients  $C_{mn}$  are dimensionless. The dimension of the operator  $\mathcal{O}_{mn}$  in (2) is  $d_{mn} = 2N + D$ , where  $D$  is the number of covariant derivatives in the operator. Since the coefficients  $C_{mn}$  take into account the effects of short distances of order  $1/m_c$ , they can be calculated as perturbation series in the QCD coupling constant  $\alpha_s(2m_c)$ . The coefficients in the perturbation series depend on  $\ln(\mu/m_c)$  in such a way as to cancel the  $\mu$ -dependence of the matrix elements.

The short-distance coefficients for annihilation decay rates can be determined by matching perturbative calculations of  $c\bar{c}$  scattering amplitudes. Let  $c\bar{c}(\mathbf{q}, \xi, \eta)$  represent a state that consists of a  $c$  and a  $\bar{c}$  with spatial momenta  $\pm\mathbf{q}$  in the  $c\bar{c}$  rest frame and spin and color states specified by the spinors  $\xi$  and  $\eta$ . The standard relativistic normalization is

$$\langle c(\mathbf{q}'_1, \xi') \bar{c}(\mathbf{q}'_2, \eta') | c(\mathbf{q}_1, \xi) \bar{c}(\mathbf{q}_2, \eta) \rangle = 4E_{q_1} E_{q_2} (2\pi)^{2N} \delta^N(\mathbf{q}_1 - \mathbf{q}'_1) \delta^N(\mathbf{q}_2 - \mathbf{q}'_2) \xi'^{\dagger} \xi \eta'^{\dagger} \eta, \quad (4)$$

where  $E_q = \sqrt{m_c^2 + \mathbf{q}^2}$ . The spinors are normalized so that  $\xi^{\dagger} \xi = 1$ , and similarly for  $\eta$ ,  $\xi'$ , and  $\eta'$ . Using the abbreviated notation  $c\bar{c} \equiv c\bar{c}(\mathbf{q}, \xi, \eta)$  and  $c\bar{c}' \equiv c\bar{c}(\mathbf{q}', \xi', \eta')$ , the matching condition in the threshold expansion method of Ref. [2] is

$$\begin{aligned} \sum_X (2\pi)^{N+1} \delta^{N+1}(P - k_X) (\mathcal{T}_{c\bar{c}' \rightarrow X})^* \mathcal{T}_{c\bar{c} \rightarrow X} \Big|_{pQCD} \\ = \sum_{mn} \frac{C_{mn}(\mu)}{m_c^{d_{mn} - N - 1}} \langle c\bar{c}' | \psi^{\dagger} \mathcal{K}'^{\dagger}_m \chi \chi^{\dagger} \mathcal{K}_n \psi | c\bar{c} \rangle^{(\mu)} \Big|_{pNRQCD}, \end{aligned} \quad (5)$$

where  $P = (2E_q, 0)$  is the momentum of the  $c\bar{c}$  pair,  $\mathcal{T}_{c\bar{c} \rightarrow X}$  is the  $T$ -matrix element for annihilation of the  $c\bar{c}$  into the state  $X$  consisting of light partons, and  $k_X$  is the sum of the momenta of the outgoing partons. The sum over  $X$  on the left side of (5) includes integration

over the phase space of the final state partons and sum over their spin and color quantum numbers. By the optical theorem, the left side of (5) is proportional to the imaginary part of the annihilation contribution to the  $T$ -matrix element  $\mathcal{T}_{c\bar{c}\rightarrow c\bar{c}'}$ . Specifically, it is the sum of all cut diagrams for which the cut does not pass through any heavy quark lines.

To carry out the matching procedure, the left side of (5) is calculated using perturbation theory in full QCD, and then expanded in powers of  $\mathbf{q}$  and  $\mathbf{q}'$ . The matrix elements on the right side of (5) are calculated using perturbation theory in NRQCD, and then expanded in powers of  $\mathbf{q}$  and  $\mathbf{q}'$ . The short-distance coefficients  $C_{mn}$  are obtained by matching the terms in the expansions in  $\mathbf{q}$  and  $\mathbf{q}'$  order by order in  $\alpha_s$ .

The calculation of the short-distance coefficients can be simplified by averaging both sides of the matching condition (5) over rotations of the vectors  $\mathbf{q}'$  and  $\mathbf{q}$  and the spinors  $\xi$ ,  $\eta$ ,  $\xi'$ , and  $\eta'$  that specify the states of the initial and final  $c\bar{c}$  pairs. On the NRQCD side of the matching equation, the average over rotations can be accomplished simply by restricting the operators  $\mathcal{O}_{mn}$  to be rotationally invariant.

In the perturbative calculations of the matching condition (5), infrared and ultraviolet divergences can appear on both sides of the equation. Since NRQCD is constructed to be equivalent to full QCD at low momenta, the infrared divergences on both sides must match. They therefore cancel in the short-distance coefficients  $C_{mn}$ . Any ultraviolet divergences on the left side are eliminated by renormalization of the QCD coupling constant and the heavy quark mass. On the right side, the ultraviolet divergences are eliminated by renormalization of the gauge coupling constant and other parameters in the NRQCD lagrangian and by renormalization of the 4-fermion operators of NRQCD.

The matching calculations are particularly simple if dimensional regularization is used to regulate both infrared and ultraviolet divergences. Radiative corrections to the NRQCD matrix elements vanish identically, because after expanding the integrand of the radiative correction in powers of  $\mathbf{q}$  and  $\mathbf{q}'$ , there is no momentum scale in the dimensionally regularized integral. The radiative corrections to the matrix elements do include infrared poles in  $\epsilon = (3-N)/2$  that match the infrared divergence on the QCD side of the matching condition,

but they are canceled by ultraviolet poles in  $\epsilon$ . Thus the only noncanceling contributions to the NRQCD side of the matching condition are the tree-level contributions of the matrix elements, including those matrix elements that arise from counterterms associated with operator renormalization.

### III. PERTURBATIVE MATCHING OF QCD AND NRQCD

In this section, we use the threshold expansion method to calculate selected terms in the short-distance coefficients in the factorization formula (1). We calculate the term proportional to  $n_f\alpha_s^2$  from the color-octet annihilation processes  $c\bar{c} \rightarrow q\bar{q}$  and the terms proportional to  $\alpha_s^2$  and  $n_f\alpha_s^3$  from the color-singlet annihilation processes  $c\bar{c} \rightarrow q\bar{q}g$  and  $c\bar{c} \rightarrow gg$ . Dimensional regularization is used as a cutoff for both infrared and ultraviolet divergences.

#### A. Color-octet terms from $c\bar{c} \rightarrow q\bar{q}$

The terms on the QCD side of the matching condition (5) that are proportional to  $n_f\alpha_s^2$  come from the annihilation process  $c\bar{c} \rightarrow q\bar{q}$ . For these terms, the left side of (5) reduces to

$$\int_{\ell_1} \int_{\ell_2} (2\pi)^{N+1} \delta^{N+1}(P - \ell_1 - \ell_2) \sum (\mathcal{T}_{c\bar{c}' \rightarrow q\bar{q}})^* \mathcal{T}_{c\bar{c} \rightarrow q\bar{q}}, \quad (6)$$

where  $\ell_1$  and  $\ell_2$  are the momenta of the  $q$  and  $\bar{q}$  and the remaining sum is over their colors, spins, and flavors. The symbol  $\int_k$  denotes the  $N$ -dimensional integral over the phase space associated with the momentum  $k$ :

$$\int_k \equiv \int \frac{d^N k}{(2\pi)^N 2k_0}. \quad (7)$$

The term in (6) that is proportional to  $n_f\alpha_s^2$  is given by the cut Feynman diagram in Figure 1. The T-matrix element for  $c(p)\bar{c}(\bar{p}) \rightarrow q(l_1)\bar{q}(l_2)$  is

$$\mathcal{T}_{c\bar{c} \rightarrow q\bar{q}} = \left( g_s \mu^\epsilon \bar{v}(\bar{p}) \gamma^\mu T^a u(p) \right) \frac{1}{4E_q^2} \left( g_s \mu^\epsilon \bar{u}(l_1) \gamma_\mu T^a v(l_2) \right). \quad (8)$$

The  $c$  and  $\bar{c}$  have 4-momenta  $p = (E_q, \mathbf{q})$  and  $\bar{p} = (E_q, -\mathbf{q})$  where  $E_q = \sqrt{m_c^2 + \mathbf{q}^2}$ . The coupling constant in (8) has been written  $g_s \mu^\epsilon$ , where  $\epsilon = (3 - N)/2$  and  $\mu$  is the scale of dimensional regularization, so that  $g_s$  remains dimensionless in  $N$  dimensions. The integrals over  $\ell_1$  and  $\ell_2$  in (6) can be carried out by using the energy-momentum-conserving delta function:

$$\begin{aligned} & \int_{\ell_1} \int_{\ell_2} (2\pi)^{N+1} \delta^{N+1}(P - \ell_1 - \ell_2) \sum \bar{v}(\ell_2) \gamma_\nu T^b u(\ell_1) \bar{u}(\ell_1) \gamma_\mu T^a v(\ell_2) \\ &= n_f \frac{(N-1) \Gamma(\frac{3}{2})}{8\pi N \Gamma(\frac{N}{2})} \left( \frac{P^2}{16\pi} \right)^{-\epsilon} \left( -P^2 g_{\mu\nu} + P_\mu P_\nu \right) \delta^{ab}, \end{aligned} \quad (9)$$

where  $P = (2E_q, \mathbf{0})$ . We have expressed this in Lorentz-invariant form for later use. Inserting this into the QCD side of the matching condition, it reduces to

$$-n_f \frac{(N-1) \Gamma(\frac{3}{2})}{32\pi N \Gamma(\frac{N}{2})} g_s^4 \mu^{4\epsilon} \left( \frac{E_q^2}{4\pi} \right)^{-\epsilon} \frac{1}{E_q^2} \bar{u}(p) \gamma^\mu T^a v(\bar{p}) \bar{v}(\bar{p}) \gamma_\mu T^a u(p). \quad (10)$$

Using the formulas in Appendix A,  $\bar{v}(\bar{p}) \gamma_\mu T^a u(p)$  can be expressed in terms of nonrelativistic Pauli spinors. Expanding to linear order in  $\mathbf{q}$ , we obtain

$$\bar{v}(\bar{p}) \gamma^\mu T^a u(p) \approx -2m_c g^{\mu i} \eta^\dagger \sigma^i T^a \xi. \quad (11)$$

The QCD side of the matching condition (10) then reduces to

$$n_f \frac{2\pi (N-1) \Gamma(\frac{3}{2})}{N \Gamma(\frac{N}{2})} \alpha_s^2 \mu^{4\epsilon} \left( \frac{m_c^2}{4\pi} \right)^{-\epsilon} \xi'^\dagger \boldsymbol{\sigma} T^a \eta' \cdot \eta^\dagger \boldsymbol{\sigma} T^a \xi. \quad (12)$$

Setting  $N = 3$ , this simplifies to

$$\frac{4\pi n_f}{3} \alpha_s^2 \xi'^\dagger \boldsymbol{\sigma} T^a \eta' \cdot \eta^\dagger \boldsymbol{\sigma} T^a \xi. \quad (13)$$

Dividing by  $(2m_c)^2$  to account for the difference in the normalization of states, we reproduce twice the leading term in  $\text{Im}\mathcal{M}$  given in (A13) of Ref. [1].

## B. Color-singlet terms from $c\bar{c} \rightarrow q\bar{q}g$

Terms proportional to  $n_f \alpha_s^3$  on the QCD side of the matching condition come from the processes  $c\bar{c} \rightarrow q\bar{q}g$  and  $c\bar{c} \rightarrow q\bar{q}$ . For the process  $c\bar{c} \rightarrow q\bar{q}g$ , the left side of (5) can be written



$$\int_k \int_{\ell_1} \int_{\ell_2} (2\pi)^{N+1} \delta^{N+1}(P - k - \ell_1 - \ell_2) \sum (\mathcal{T}_{c\bar{c}' \rightarrow q\bar{q}g})^* \mathcal{T}_{c\bar{c} \rightarrow q\bar{q}g}, \quad (14)$$

where  $\ell_1$ ,  $\ell_2$ , and  $k$  are the momenta of the  $q$ ,  $\bar{q}$ , and gluon, respectively, and the remaining sum is over the colors, spins, and flavors of these partons. The term proportional to  $n_f \alpha_s^3$  comes from the cut Feynman diagrams in Figure 2. The T-matrix element in Feynman gauge for  $c(p)\bar{c}(\bar{p}) \rightarrow q(l_1)\bar{q}(l_2)g(k)$  can be written

$$\mathcal{T}_{c\bar{c} \rightarrow q\bar{q}g} = \mathcal{A}_{c\bar{c} \rightarrow g^*g}^{\mu a} \frac{1}{(\ell_1 + \ell_2)^2} \left( g_s \mu^\epsilon \bar{u}(l_1) \gamma_\mu T^a v(l_2) \right), \quad (15)$$

where  $\mathcal{A}_{c\bar{c} \rightarrow g^*g}^{\mu a}$  is the amplitude for the process  $c(p) \bar{c}(\bar{p}) \rightarrow g^*(l)g(k)$ :

$$\begin{aligned} \mathcal{A}_{c\bar{c} \rightarrow g^*g}^{\mu a} = g_s^2 \mu^{2\epsilon} \epsilon_\nu^b(k) \bar{v}(\bar{p}) \left[ \frac{\gamma^\nu (\not{k} - \not{p} + m_c) \gamma^\mu}{2\bar{p} \cdot k} T^b T^a \right. \\ \left. + \frac{\gamma^\mu (\not{p} - \not{k} + m_c) \gamma^\nu}{2p \cdot k} T^a T^b \right] u(p). \end{aligned} \quad (16)$$

We will compute the matching condition for the case of color-singlet  $c\bar{c}$  pairs. The color matrices  $T^a T^b$  and  $T^b T^a$  in (16) can then be replaced by  $\delta^{ab}/6$ . We will further simplify the matching condition by averaging the initial state  $c\bar{c}(\mathbf{q}, \xi, \eta)$  and the final state  $c\bar{c}(\mathbf{q}', \xi', \eta')$  over the rotation group.

The integral over  $\ell_1$  and  $\ell_2$  in (14) can be carried out by inserting the identity

$$\int \frac{d\ell^2}{2\pi} \int_\ell (2\pi)^{N+1} \delta^{N+1}(\ell - \ell_1 - \ell_2) = 1. \quad (17)$$

After using (9) with  $P$  replaced by  $\ell$  to integrate over  $\ell_1$  and  $\ell_2$ , we obtain

$$\begin{aligned} n_f \frac{(N-1)\Gamma(\frac{3}{2})}{8\pi N\Gamma(\frac{N}{2})} g_s^2 \mu^{2\epsilon} \int \frac{d\ell^2}{2\pi} \int_\ell \int_k (2\pi)^{N+1} \delta^{N+1}(P - \ell - k) \\ \times \frac{1}{(\ell^2)^2} \left( \frac{\ell^2}{16\pi} \right)^{-\epsilon} (-\ell^2 g_{\mu\nu} + \ell_\mu \ell_\nu) \sum (\mathcal{A}_{c\bar{c}' \rightarrow g^*g}^{\nu a})^* \mathcal{A}_{c\bar{c} \rightarrow g^*g}^{\mu a}. \end{aligned} \quad (18)$$

The remaining sum is over the colors and spins of the real gluon. The  $\ell_\mu \ell_\nu$  term gives no contribution due to current conservation.

We proceed to carry out the nonrelativistic expansion of the factor in (18) that involves the amplitude  $\mathcal{A}_{c\bar{c} \rightarrow g^*g}^{\mu a}$ . Using the identities in Appendix A, we expand (16) to linear order in  $\mathbf{q}$ :

$$\begin{aligned}
\mathcal{A}_{c\bar{c}\rightarrow g^*g}^{\mu a} &= \frac{g_s^2 \mu^{2\epsilon}}{12m_c k_0} \epsilon_\nu^a(k) \left\{ m_c g^{\mu i} g^{\nu j} \eta^\dagger \{[\sigma^i, \sigma^j], \mathbf{k} \cdot \boldsymbol{\sigma}\} \xi \right. \\
&\quad + 4 \left[ \frac{1}{k_0} k^i \left( k^\mu g^{\nu j} + g^{\mu j} k^\nu - 2m_c g^{\mu j} g^{\nu 0} - k^j g^{\mu\nu} \right) \right. \\
&\quad \quad - k^i (g^{\mu 0} g^{\nu j} - g^{\nu 0} g^{\mu j}) + k^j (g^{\mu 0} g^{\nu i} - g^{\nu 0} g^{\mu i}) \\
&\quad \quad \left. \left. + k_0 g^{\mu i} g^{\nu j} + (2m_c - k_0) g^{\mu j} g^{\nu i} \right] \eta^\dagger q^i \sigma^j \xi \right\}. \quad (19)
\end{aligned}$$

In  $N > 3$  dimensions, the spin matrix  $\{[\sigma^i, \sigma^j], \sigma^k\}$ , which is totally antisymmetric in its three indices, is linearly independent of 1 and  $\sigma^i, i = 1, \dots, N$ . In 3 dimensions, it reduces to the unit matrix multiplied by  $-4i\epsilon^{ijk}$ .

After multiplying  $\mathcal{A}_{c\bar{c}\rightarrow g^*g}^{\mu a}$  by  $(\mathcal{A}_{c\bar{c}\rightarrow g^*g}^{\nu a})^*$ , the spinor factors can be simplified by averaging the vectors  $\mathbf{q}$  and  $\mathbf{q}'$  and the spinors  $\xi, \eta, \xi'$ , and  $\eta'$  over the rotation group. The factor  $\xi'^\dagger q'^k \sigma^l \eta' \eta^\dagger q^i \sigma^j \xi$  reduces to a linear combination of three independent spinor factors:

$$\begin{aligned}
\overline{\xi'^\dagger q'^k \sigma^l \eta' \eta^\dagger q^i \sigma^j \xi} &= \frac{1}{N(N-1)(N+2)} \\
&\times \left[ \left( (N+1)\delta^{ij}\delta^{kl} - \delta^{ik}\delta^{jl} - \delta^{il}\delta^{jk} \right) \xi'^\dagger \mathbf{q}' \cdot \boldsymbol{\sigma} \eta' \eta^\dagger \mathbf{q} \cdot \boldsymbol{\sigma} \xi \right. \\
&\quad + \left( (N+1)\delta^{ik}\delta^{jl} - \delta^{ij}\delta^{kl} - \delta^{il}\delta^{jk} \right) \xi'^\dagger q'^m \sigma^n \eta' \eta^\dagger q^m \sigma^n \xi \\
&\quad \left. + \left( (N+1)\delta^{il}\delta^{jk} - \delta^{ij}\delta^{kl} - \delta^{ik}\delta^{jl} \right) \xi'^\dagger q'^m \sigma^n \eta' \eta^\dagger q^n \sigma^m \xi \right]. \quad (20)
\end{aligned}$$

The spinor factors  $\xi'^\dagger q'^l \sigma^m \eta' \eta^\dagger \{[\sigma^i, \sigma^j], \sigma^k\} \xi$  and  $\xi'^\dagger \{[\sigma^l, \sigma^m], \sigma^n\} \eta' \eta^\dagger q^i \sigma^j \xi$  average to zero, while  $\xi'^\dagger \{[\sigma^l, \sigma^m], \sigma^n\} \eta' \eta^\dagger \{[\sigma^i, \sigma^j], \sigma^k\} \xi$  reduces to a single spinor factor:

$$\begin{aligned}
&\overline{\xi'^\dagger \{[\sigma^l, \sigma^m], \sigma^n\} \eta' \eta^\dagger \{[\sigma^i, \sigma^j], \sigma^k\} \xi} \\
&= \frac{1}{N(N-1)(N-2)} \begin{vmatrix} \delta^{il} & \delta^{jl} & \delta^{kl} \\ \delta^{im} & \delta^{jm} & \delta^{km} \\ \delta^{in} & \delta^{jn} & \delta^{kn} \end{vmatrix} \xi'^\dagger \{[\sigma^r, \sigma^s], \sigma^t\} \eta' \eta^\dagger \{[\sigma^r, \sigma^s], \sigma^t\} \xi. \quad (21)
\end{aligned}$$

In 3 space dimensions, the spinor factor on the right side of (21) can be simplified by using the commutation relations of the Pauli matrices:

$$\xi'^\dagger \{[\sigma^r, \sigma^s], \sigma^t\} \eta' \eta^\dagger \{[\sigma^r, \sigma^s], \sigma^t\} \xi = -96 \xi'^\dagger \eta' \eta^\dagger \xi, \quad N = 3. \quad (22)$$

However this simplification can only be made if there are no poles in  $N - 3$  multiplying the spinor factor. After averaging over the rotation group using (20) and (21) and simplifying the Lorentz algebra, we obtain

$$\begin{aligned}
(-g_{\mu\nu}) \sum \overline{\left(\mathcal{A}_{c\bar{c}' \rightarrow g^*g}^{\nu a}\right)^* \mathcal{A}_{c\bar{c} \rightarrow g^*g}^{\mu a}} &= \frac{128\pi^2}{9N(N+2)} \alpha_s^2 \mu^{4\epsilon} \frac{1}{x^2} \\
&\times \left( 6(N+2)x^2 \left(-\frac{1}{96} \xi'^{\dagger} \{[\sigma^r, \sigma^s], \sigma^t\} \eta' \eta^{\dagger} \{[\sigma^r, \sigma^s], \sigma^t\} \xi\right) \right. \\
&\quad + \left[ 4(N+2)x + (N-1)x^2 \right] \frac{1}{m_c^2} \xi'^{\dagger} \mathbf{q}' \cdot \boldsymbol{\sigma} \eta' \eta^{\dagger} \mathbf{q} \cdot \boldsymbol{\sigma} \xi \\
&\quad + \left[ 4(N+2)(N-1)(1-x) + (2N^2 + N - 9)x^2 \right] \frac{1}{m_c^2} \xi'^{\dagger} q'^m \sigma^n \eta' \eta^{\dagger} q^m \sigma^n \xi \\
&\quad \left. + \left[ 4(N+2)(N-2)x - (2N^2 - N - 7)x^2 \right] \frac{1}{m_c^2} \xi'^{\dagger} q'^m \sigma^n \eta' \eta^{\dagger} q^n \sigma^m \xi \right), \quad (23)
\end{aligned}$$

where  $x = k_0/m_c$ .

At this point, the integrand of (18) has been reduced to a function of  $\ell^2 = 4E_q(E_q - k_0)$ .

We can therefore carry out the phase space integral over  $k$  and  $\ell$ :

$$\int_{\ell} \int_k (2\pi)^{N+1} \delta^{N+1}(P - \ell - k) = \frac{\Gamma(\frac{3}{2})}{8\pi\Gamma(\frac{N}{2})} \left(\frac{P^2}{16\pi}\right)^{\frac{N-3}{2}} \left(\frac{P^2 - \ell^2}{P^2}\right)^{N-2}. \quad (24)$$

Changing the integration variable to  $x = 1 - \ell^2/(4E_q^2)$  and taking the nonrelativistic limit, the QCD side of the matching condition reduces to

$$\begin{aligned}
n_f \frac{(N-1)\Gamma^2(\frac{3}{2})}{32\pi^2 N \Gamma^2(\frac{N}{2})} \alpha_s \mu^{2\epsilon} \left(\frac{m_c^2}{4\pi}\right)^{-2\epsilon} \int_0^1 dx x^{1-2\epsilon} (1-x)^{-1-\epsilon} \\
\times (-g_{\mu\nu}) \sum \left(\mathcal{A}_{c\bar{c}' \rightarrow g^*g}^{\nu a}\right)^* \mathcal{A}_{c\bar{c} \rightarrow g^*g}^{\mu a}. \quad (25)
\end{aligned}$$

Infrared divergences arise from the endpoints of the integral in (25). The infrared divergences from  $x \rightarrow 1$  arise when the  $q$  and  $\bar{q}$  are collinear with the virtual gluon, which is almost on-shell. They are canceled by collinear infrared divergences from radiative correction to the process  $c\bar{c} \rightarrow gg$ , which will be calculated in subsection IIIC. The infrared divergence from  $x \rightarrow 0$ , which appears only in the coefficient of  $\xi'^{\dagger} q'^m \sigma^n \eta' \eta^{\dagger} q^m \sigma^n \xi$ , arises when the emitted real gluon is soft. It must be matched by an infrared divergence on the NRQCD side of the matching condition. The analytic expressions for the integrals over  $x$  is

$$\int_0^1 dx x^{n-1-2\epsilon}(1-x)^{-1-\epsilon} = \frac{\Gamma(n-2\epsilon)\Gamma(-\epsilon)}{\Gamma(n-3\epsilon)}. \quad (26)$$

Integrating over  $x$  and keeping only the terms that survive in the limit  $\epsilon \rightarrow 0$ , we obtain

$$\begin{aligned} n_f \frac{4(N-1)\Gamma^2(\frac{3}{2})}{9N^2(N+2)\Gamma^2(\frac{N}{2})} \alpha_s^3 \mu^{6\epsilon} \left(\frac{m_c^2}{4\pi}\right)^{-2\epsilon} \\ \times \frac{1}{\epsilon_{IR}} \left[ -6(5+3\epsilon) \left(-\frac{1}{96} \xi'^{\dagger} \{[\sigma^r, \sigma^s], \sigma^t\} \eta' \eta^{\dagger} \{[\sigma^r, \sigma^s], \sigma^t\} \xi\right) \right. \\ - 2(11-4\epsilon) \frac{1}{m_c^2} \xi'^{\dagger} \mathbf{q}' \cdot \boldsymbol{\sigma} \eta' \eta^{\dagger} \mathbf{q} \cdot \boldsymbol{\sigma} \xi \\ - 2(16-21\epsilon) \frac{1}{m_c^2} \xi'^{\dagger} q'^m \sigma^n \eta' \eta^{\dagger} q^m \sigma^n \xi \\ \left. - 2(6-17\epsilon) \frac{1}{m_c^2} \xi'^{\dagger} q'^m \sigma^n \eta' \eta^{\dagger} q^n \sigma^m \xi \right]. \quad (27) \end{aligned}$$

The subscript  $IR$  on the pole in  $\epsilon$  is a reminder that it has an infrared origin.

### C. Color-singlet terms from $c\bar{c} \rightarrow gg$

The remaining terms on the QCD side of the matching condition that are proportional to  $n_f \alpha_s^3$  come from the process  $c\bar{c} \rightarrow gg$ . For this process, the QCD side of the matching condition (5) reduces to

$$\frac{1}{2} \int_k \int_{\ell} (2\pi)^{N+1} \delta^{N+1}(P-k-\ell) \sum (\mathcal{T}_{c\bar{c}' \rightarrow gg})^* \mathcal{T}_{c\bar{c} \rightarrow gg}, \quad (28)$$

where  $k$  and  $\ell$  are the momenta of the gluons, the sum is over their spins and colors, and the factor of  $\frac{1}{2}$  comes from Bose statistics.

We first consider the QCD side of the matching condition at leading order in  $\alpha_s$ . At this order, it is given by the cut Feynman diagrams in Figure 3. The  $T$ -matrix element for  $c(p)\bar{c}(\bar{p}) \rightarrow g(k)g(l)$  is

$$\mathcal{T}_{c\bar{c} \rightarrow gg} = \mathcal{A}_{c\bar{c} \rightarrow gg}^{\mu a} \epsilon_{\mu}^a(\ell), \quad (29)$$

where  $\mathcal{A}_{c\bar{c} \rightarrow gg}^{\mu a}$  is identical to (16) except that  $\ell^2 = 0$ . The nonrelativistic expansion of the matching condition is similar to but simpler than that for  $c\bar{c} \rightarrow q\bar{q}g$ , which was carried out in subsection IIIB. The final result is

$$\begin{aligned}
& \frac{8\pi\Gamma(\frac{3}{2})}{9N(N+2)\Gamma(\frac{N}{2})} \alpha_s^2 \mu^{4\epsilon} \left(\frac{m_c^2}{4\pi}\right)^{-\epsilon} \\
& \times \left[ 6(N+2) \left(-\frac{1}{96}\xi'^\dagger\{[\sigma^r, \sigma^s], \sigma^t\}\eta'\eta^\dagger\{[\sigma^r, \sigma^s], \sigma^t\}\xi\right) \right. \\
& \quad + (5N+7) \frac{1}{m_c^2} \xi'^\dagger \mathbf{q}' \cdot \boldsymbol{\sigma} \eta' \eta^\dagger \mathbf{q} \cdot \boldsymbol{\sigma} \xi \\
& \quad \left. + (2N^2 + N - 9) \frac{1}{m_c^2} \xi'^\dagger q'^m \sigma^n \eta' \eta^\dagger (q^m \sigma^n + q^n \sigma^m) \xi \right]. \quad (30)
\end{aligned}$$

Setting  $N = 3$ , this simplifies to

$$\begin{aligned}
& \frac{16\pi}{135} \alpha_s^2 \left[ 15 \xi'^\dagger \eta' \eta^\dagger \xi + 11 \frac{1}{m_c^2} \xi'^\dagger \mathbf{q}' \cdot \boldsymbol{\sigma} \eta' \eta^\dagger \mathbf{q} \cdot \boldsymbol{\sigma} \xi \right. \\
& \quad \left. + 6 \frac{1}{m_c^2} \xi'^\dagger q'^m \sigma^n \eta' \eta^\dagger (q^m \sigma^n + q^n \sigma^m) \xi \right]. \quad (31)
\end{aligned}$$

Dividing by  $(2m_c)^2$  to account for the difference in the normalization of states, we reproduce twice the corresponding terms in  $\text{Im}\mathcal{M}$  given by the sum of (A9a) and (A9b) of Ref. [1].

The terms in (28) proportional to  $n_f \alpha_s^3$  come from the renormalization of the coupling constant in (30) and from the cuts of the Feynman diagrams in Figure 2 that pass through 2 gluon lines. The renormalization contribution in the  $\overline{MS}$  prescription is obtained by multiplying (30) by  $Z_g^4$ , where

$$Z_g = 1 + \frac{n_f}{12\pi} \alpha_s \left( \frac{1}{\epsilon_{UV}} + \ln(4\pi) - \gamma \right). \quad (32)$$

The subscript  $UV$  on the pole in  $\epsilon$  is a reminder that it has an ultraviolet origin. In the diagrams obtained by cutting two gluon lines in Figure 2, the quark loops have ultraviolet divergences and collinear infrared divergences. With dimensional regularization, there is a cancellation between the ultraviolet and infrared divergences and the diagrams vanish. Making this cancellation explicit, the sum of the diagrams can be expressed as (30) multiplied by the factor

$$-\frac{n_f}{3\pi} \alpha_s \left( \frac{1}{\epsilon_{UV}} - \frac{1}{\epsilon_{IR}} \right). \quad (33)$$

The ultraviolet pole in  $\epsilon$  is cancelled by the renormalization factor (32). Adding the two contributions proportional to  $n_f \alpha_s^3$ , we obtain

$$\begin{aligned}
n_f \frac{8\Gamma(\frac{3}{2})}{27N(N+2)\Gamma(\frac{N}{2})} \alpha_s^3 \mu^{4\epsilon} \left(\frac{m_c^2}{4\pi}\right)^{-\epsilon} & \left(\frac{1}{\epsilon_{IR}} + \ln(4\pi) - \gamma\right) \\
& \times \left[ 6(N+2) \left(-\frac{1}{96} \xi'^{\dagger} \{[\sigma^r, \sigma^s], \sigma^t\} \eta' \eta^{\dagger} \{[\sigma^r, \sigma^s], \sigma^t\} \xi\right) \right. \\
& + (5N+7) \frac{1}{m_c^2} \xi'^{\dagger} \mathbf{q}' \cdot \boldsymbol{\sigma} \eta' \eta^{\dagger} \mathbf{q} \cdot \boldsymbol{\sigma} \xi \\
& \left. + (2N^2 + N - 9) \frac{1}{m_c^2} \xi'^{\dagger} q'^m \sigma^n \eta' \eta^{\dagger} (q^m \sigma^n + q^n \sigma^m) \xi \right]. \quad (34)
\end{aligned}$$

On the QCD side of the matching condition, the total contribution proportional to  $n_f \alpha_s^3$  is the sum of (27) and (34). The pole in  $\epsilon$  in front of the spinor factor  $\xi'^{\dagger} \{[\sigma^r, \sigma^s], \sigma^t\} \eta' \eta^{\dagger} \{[\sigma^r, \sigma^s], \sigma^t\} \xi$  cancels in the sum. The spinor factor can therefore be simplified using (22). Adding (27) and (34) and keeping only the terms that survive in the limit  $\epsilon \rightarrow 0$ , we obtain

$$\begin{aligned}
n_f \frac{8\Gamma(\frac{3}{2})}{27N(N+2)\Gamma(\frac{N}{2})} \alpha_s^3 \mu^{4\epsilon} \left(\frac{m_c^2}{4\pi}\right)^{-\epsilon} & \left\{ -60 \left(\ln \frac{\mu}{2m_c} + \frac{4}{3}\right) \xi'^{\dagger} \eta' \eta^{\dagger} \xi \right. \\
& - 44 \left(\ln \frac{\mu}{2m_c} + \frac{29}{33}\right) \frac{1}{m_c^2} \xi'^{\dagger} \mathbf{q}' \cdot \boldsymbol{\sigma} \eta' \eta^{\dagger} \mathbf{q} \cdot \boldsymbol{\sigma} \xi \\
& + \left[-20 \left(\frac{1}{\epsilon_{IR}} + \ln(4\pi) - \gamma\right) - 64 \left(\ln \frac{\mu}{2m_c} + \frac{7}{12}\right)\right] \frac{1}{m_c^2} \xi'^{\dagger} q'^m \sigma^n \eta' \eta^{\dagger} q^m \sigma^n \xi \\
& \left. - 24 \left(\ln \frac{\mu}{2m_c} + \frac{1}{2}\right) \frac{1}{m_c^2} \xi'^{\dagger} q'^m \sigma^n \eta' \eta^{\dagger} q^n \sigma^m \xi \right\}. \quad (35)
\end{aligned}$$

#### D. Short-distance coefficients

We now calculate the matrix elements that must appear on the NRQCD side of the matching condition (5) and extract their short-distance coefficients. We will find that the terms that are required for matching are

$$\begin{aligned}
\frac{C^{(\underline{1},^1S)}}{m_c^{N-1}} \langle c\bar{c}' | \psi^{\dagger} \chi \chi^{\dagger} \psi | c\bar{c} \rangle & + \frac{C^{(\underline{8},^3S)}}{m_c^{N-1}} \langle c\bar{c}' | \psi^{\dagger} \boldsymbol{\sigma} T^a \chi \cdot \chi^{\dagger} \boldsymbol{\sigma} T^a \psi | c\bar{c} \rangle^{(\mu)} \\
& + \frac{C_1^{(\underline{1},^3P)}}{m_c^{N+1}} \langle c\bar{c}' | \psi^{\dagger} (-\frac{i}{2} \overleftrightarrow{\mathbf{D}} \cdot \boldsymbol{\sigma}) \chi \chi^{\dagger} (-\frac{i}{2} \overleftrightarrow{\mathbf{D}} \cdot \boldsymbol{\sigma}) \psi | c\bar{c} \rangle \\
& + \frac{C_2^{(\underline{1},^3P)}(\mu)}{m_c^{N+1}} \langle c\bar{c}' | \psi^{\dagger} (-\frac{i}{2} \overleftrightarrow{D})^m \sigma^n \chi \chi^{\dagger} (-\frac{i}{2} \overleftrightarrow{D})^m \sigma^n \psi | c\bar{c} \rangle \\
& + \frac{C_3^{(\underline{1},^3P)}}{m_c^{N+1}} \langle c\bar{c}' | \psi^{\dagger} (-\frac{i}{2} \overleftrightarrow{D})^m \sigma^n \chi \chi^{\dagger} (-\frac{i}{2} \overleftrightarrow{D})^n \sigma^m \psi | c\bar{c} \rangle + \dots \quad (36)
\end{aligned}$$

We have placed a superscript ( $\mu$ ) on the color-octet matrix element in anticipation of the fact that it will acquire dependence on the NRQCD renormalization scale through renormalization.

We consider the matching condition first for color-octet  $c\bar{c}$  pairs and then for color-singlet  $c\bar{c}$  pairs. In the case of color-octet  $c\bar{c}$  pairs, the contribution proportional to  $n_f\alpha_s^2$  on the QCD side of the matching condition is given in (12). The spinor factor in (12) can be identified as the expression at leading order in  $\alpha_s$  and expanded to linear order in  $\mathbf{q}$  and  $\mathbf{q}'$  of the following NRQCD matrix element:

$$\langle c\bar{c}' | \psi^\dagger \boldsymbol{\sigma} T^a \chi \cdot \chi^\dagger \boldsymbol{\sigma} T^a \psi | c\bar{c} \rangle \approx 4m_c^2 \xi'^\dagger \boldsymbol{\sigma} T^a \eta' \cdot \eta^\dagger \boldsymbol{\sigma} T^a \xi . \quad (37)$$

The tree-level expression for the matrix element in (37) is represented diagrammatically in Fig. 4, with the dot representing the operator. Comparing (12) and (36), we can read off the short-distance coefficient of the matrix element in (37):

$$C^{(\mathbb{8},^3S)} = n_f \frac{\pi(N-1)\Gamma(\frac{3}{2})}{2N\Gamma(\frac{N}{2})} \alpha_s^2 \left( \frac{4\pi\mu^4}{m_c^4} \right)^\epsilon . \quad (38)$$

Taking the limit  $N \rightarrow 3$ , this reduces to

$$C^{(\mathbb{8},^3S)} = \frac{\pi n_f}{3} \alpha_s^2 (2m_c) . \quad (39)$$

Since the short-distance coefficient is sensitive only to momenta of order  $m_c$ , we have set the scale of the running coupling constant to  $\mu = 2m_c$ .

In the case of color-singlet  $c\bar{c}$  pairs, the contributions proportional to  $\alpha_s^2$  and  $n_f\alpha_s^3$  on the QCD side of the matching condition are given in (31) and (35), respectively. The spinor factors in these expressions can be identified as tree-level expressions for NRQCD matrix elements, expanded to linear order in  $\mathbf{q}$  and  $\mathbf{q}'$ . The S-wave spinor factor is proportional to

$$\langle c\bar{c}' | \psi^\dagger \chi \chi^\dagger \psi | c\bar{c} \rangle \approx 4m_c^2 \xi'^\dagger \eta' \eta^\dagger \xi . \quad (40)$$

Comparing the sum of (31) and (35) with (36), we can read off the short-distance coefficient of the matrix element in (40):

$$C^{(\underline{1},^1S)} = \frac{4\pi}{9}\alpha_s^2(\mu) \left[ 1 + \left( -\frac{2}{3} \ln \frac{\mu}{2m_c} - \frac{8}{9} \right) n_f \frac{\alpha_s}{\pi} \right]. \quad (41)$$

Choosing the QCD renormalization scale to be  $\mu = 2m_c$ , this reduces to

$$C^{(\underline{1},^1S)} = \frac{4\pi}{9}\alpha_s^2(2m_c) \left( 1 - \frac{8n_f}{9} \frac{\alpha_s}{\pi} \right). \quad (42)$$

The P-wave spinor factors in (31) and (35) can be identified with the matrix elements

$$\langle c\bar{c}' | \psi^\dagger(-\frac{i}{2}\overleftrightarrow{\mathbf{D}} \cdot \boldsymbol{\sigma}) \chi \chi^\dagger(-\frac{i}{2}\overleftrightarrow{\mathbf{D}} \cdot \boldsymbol{\sigma}) \psi | c\bar{c} \rangle \approx 4m_c^2 \xi^{\dagger} \mathbf{q}' \cdot \boldsymbol{\sigma} \eta' \eta^\dagger \mathbf{q} \cdot \boldsymbol{\sigma} \xi, \quad (43a)$$

$$\langle c\bar{c}' | \psi^\dagger(-\frac{i}{2}\overleftrightarrow{D})^m \sigma^n \chi \chi^\dagger(-\frac{i}{2}\overleftrightarrow{D})^m \sigma^n \psi | c\bar{c} \rangle \approx 4m_c^2 \xi^{\dagger} q'^m \sigma^n \eta' \eta^\dagger q^m \sigma^n \xi, \quad (43b)$$

$$\langle c\bar{c}' | \psi^\dagger(-\frac{i}{2}\overleftrightarrow{D})^m \sigma^n \chi \chi^\dagger(-\frac{i}{2}\overleftrightarrow{D})^n \sigma^m \psi | c\bar{c} \rangle \approx 4m_c^2 \xi^{\dagger} q'^m \sigma^n \eta' \eta^\dagger q^n \sigma^m \xi. \quad (43c)$$

For the matrix elements (43a) and (43c), we can immediately read off the short-distance coefficients by comparing the sum of (31) and (35) with (36). Setting  $N = 3$  and  $\mu = 2m_c$ , we obtain

$$C_1^{(\underline{1},^3P)} = \frac{44\pi}{135}\alpha_s^2(2m_c) \left( 1 - \frac{58n_f}{99} \frac{\alpha_s}{\pi} \right), \quad (44)$$

$$C_3^{(\underline{1},^3P)} = \frac{8\pi}{45}\alpha_s^2(2m_c) \left( 1 - \frac{n_f}{3} \frac{\alpha_s}{\pi} \right). \quad (45)$$

The coefficient of the matrix element in (43a) is more complicated because the coefficient of  $\xi^{\dagger} q'^m \sigma^n \eta' \eta^\dagger q^m \sigma^n \xi$  in (35) contains an infrared pole in  $\epsilon$ , indicating that it is sensitive to long-distance effects. Since an infrared divergence cannot appear in a short-distance coefficient, that divergence must be matched by an infrared divergence in a radiative correction to a matrix element on the NRQCD side of the matching condition. Since the divergence in (35) has a coefficient proportional to  $n_f \alpha_s^3$ , the infrared-divergent NRQCD matrix element must have a short-distance coefficient proportional to  $n_f \alpha_s^2$ . The only such matrix element is  $\langle c\bar{c}' | \psi^\dagger \boldsymbol{\sigma} T^a \chi \cdot \chi^\dagger \boldsymbol{\sigma} T^a \psi | c\bar{c} \rangle$ , whose short-distance coefficient has already been determined in (38). Thus the infrared divergence on the NRQCD side of the matching condition must come from that term.

If the initial and final  $c\bar{c}$  pairs are in color-singlet states, the tree level expression (37) for the matrix element vanishes and the leading contribution comes instead from radiative



corrections. The leading contributions to the matrix element are represented by the diagrams in Figure 5. The expression for diagram 5a is

$$4g^2\mu^{2\epsilon} \xi'^{\dagger} \sigma^n T^a T^b \eta' \eta^{\dagger} \sigma^n T^b T^a \xi \int \frac{d^N k}{(2\pi)^N 2k} \left( \mathbf{q} \cdot \mathbf{q}' - \mathbf{q} \cdot \hat{\mathbf{k}} \hat{\mathbf{k}} \cdot \mathbf{q}' \right) \times \frac{1}{E_q - k - (\mathbf{q} - \mathbf{k})^2 / (2m_c) + i\epsilon} \frac{1}{E_q - k - (\mathbf{q}' - \mathbf{k})^2 / (2m_c) + i\epsilon}, \quad (46)$$

where  $E_q = \mathbf{q}^2 / (2m_c) = (\mathbf{q}')^2 / (2m_c)$ . Since the initial and final  $c\bar{c}$  pairs are both color-singlets, we can replace  $T^a T^b$  and  $T^b T^a$  by  $\delta^{ab} / 6$ . The proper way to evaluate the diagram is to regard  $|\mathbf{q}|$ ,  $|\mathbf{q}'|$ , and  $|\mathbf{k}|$  to all be much smaller than  $m_c$ . We must therefore expand out the denominators of (46) in powers of  $\mathbf{q}/m_c$ ,  $\mathbf{q}'/m_c$ , and  $\mathbf{k}/m_c$  before integrating over  $\mathbf{k}$ . Keeping only terms up to linear order in  $\mathbf{q}/m_c$  and  $\mathbf{q}'/m_c$ , the diagram reduces to

$$\frac{16\pi}{9} \alpha_s \mu^{2\epsilon} \xi'^{\dagger} \sigma^n \eta' \eta^{\dagger} \sigma^n \xi \int \frac{d^N k}{(2\pi)^N} \frac{\mathbf{q} \cdot \mathbf{q}' - \mathbf{q} \cdot \hat{\mathbf{k}} \hat{\mathbf{k}} \cdot \mathbf{q}'}{k^3}. \quad (47)$$

The integral is both ultraviolet and infrared divergent. It vanishes in dimensional regularization due to a cancellation between an ultraviolet pole in  $\epsilon$  and an infrared pole. Making these poles explicit, the diagram can be written

$$\frac{8}{27\pi} \alpha_s \left( \frac{1}{\epsilon_{UV}} - \frac{1}{\epsilon_{IR}} \right) \xi'^{\dagger} q^m \sigma^n \eta' \eta^{\dagger} q^m \sigma^n \xi. \quad (48)$$

The subscripts  $UV$  and  $IR$  on  $\epsilon$  indicate whether the pole is of ultraviolet or infrared origin. We have set  $N = 3$  in the prefactor, since any finite terms obtained by expanding the prefactor in powers of  $\epsilon$  will cancel. The other 3 diagrams in Figure 5 give identical contributions. The final result for the matrix element is

$$\langle c\bar{c}' | \psi^{\dagger} \boldsymbol{\sigma} T^a \chi \cdot \chi^{\dagger} \boldsymbol{\sigma} T^a \psi | c\bar{c} \rangle = \frac{32\alpha_s}{27\pi} \left( \frac{1}{\epsilon_{UV}} - \frac{1}{\epsilon_{IR}} \right) \xi'^{\dagger} q^m \sigma^n \eta' \eta^{\dagger} q^m \sigma^n \xi. \quad (49)$$

After multiplying by  $C^{(\mathbb{S}^1 S)} / m_c^{N-1}$ , where  $C^{(\mathbb{S}^1 S)}$  is given in (38), we find that the infrared pole in  $\epsilon$  matches the one on the QCD side of the matching condition, which is given in (35).

The ultraviolet pole in  $\epsilon$  in (49) indicates that the matrix element is ultraviolet divergent and therefore requires renormalization. It is the renormalized matrix element that appears in the NRQCD side of the matching condition (36). In the  $\overline{MS}$  renormalization scheme, the relation between matrix elements of the bare operator and renormalized operators is

$$\begin{aligned} \langle c\bar{c}'|\psi^\dagger\boldsymbol{\sigma}T^a\chi\cdot\chi^\dagger\boldsymbol{\sigma}T^a\psi|c\bar{c}\rangle &= \mu^{-4\epsilon}\left(\langle c\bar{c}'|\psi^\dagger\boldsymbol{\sigma}T^a\chi\cdot\chi^\dagger\boldsymbol{\sigma}T^a\psi|c\bar{c}\rangle^{(\mu)}\right. \\ &\left. + \frac{8\alpha_s}{27\pi m_c^2}\left(\frac{1}{\epsilon_{UV}} + \ln(4\pi) - \gamma\right)\langle c\bar{c}'|\psi^\dagger(-\frac{i}{2}\overleftrightarrow{D})^m\sigma^n\chi\chi^\dagger(-\frac{i}{2}\overleftrightarrow{D})^m\sigma^n\psi|c\bar{c}\rangle^{(\mu)}\right). \end{aligned} \quad (50)$$

The superscripts  $(\mu)$  on the matrix elements on the right side indicate that they are renormalized matrix elements with renormalization scale  $\mu$ . We will suppress this superscript on color-singlet matrix elements, since they do not require any renormalization at this order in  $\alpha_s$ . The fermion field operators in the bare matrix element on the left side of (50) have dimension  $N/2$ . The fermion field operators in the renormalized matrix elements on the right side have dimension  $3/2$ . The factor of  $\mu^{-4\epsilon}$  on the right side of (50) compensates for the difference between the dimensions of the two sides. Solving (50) for  $\langle c\bar{c}'|\psi^\dagger\boldsymbol{\sigma}T^a\chi\cdot\chi^\dagger\boldsymbol{\sigma}T^a|c\bar{c}\rangle^{(\mu)}$  and using (49) and (43b), we find that the renormalized matrix element is

$$\langle c\bar{c}'|\psi^\dagger\boldsymbol{\sigma}T^a\chi\cdot\chi^\dagger\boldsymbol{\sigma}T^a\psi|c\bar{c}\rangle^{(\mu)} = -\frac{32}{27\pi}\alpha_s\left(\frac{1}{\epsilon_{IR}} + \ln(4\pi) - \gamma\right)\xi'^\dagger q'^m\sigma^n\eta'\eta^\dagger q^m\sigma^n\xi. \quad (51)$$

Multiplying by  $C^{(\mathbb{S}^1S)}/m_c^{N-1}$ , where  $C^{(\mathbb{S}^1S)}$  is given in (38) and keeping all terms that survive in the limit  $\epsilon \rightarrow 0$ , we find that the contribution to the NRQCD side of the matching condition is

$$\begin{aligned} \frac{C^{(\mathbb{S}^3S)}}{m_c^{N-1}}\langle c\bar{c}'|\psi^\dagger\boldsymbol{\sigma}T^a\chi\cdot\chi^\dagger\boldsymbol{\sigma}T^a\psi|c\bar{c}\rangle^{(\mu)} &= n_f\frac{8\Gamma(\frac{3}{2})}{27N(N+2)\Gamma(\frac{N}{2})}\alpha_s^3\mu^{4\epsilon}\left(\frac{m_c^2}{4\pi}\right)^{-\epsilon} \\ &\times\left[-20\left(\frac{1}{\epsilon_{IR}} + \ln(4\pi) - \gamma - \frac{7}{5}\right)\right]\frac{1}{m_c^2}\xi'^\dagger q'^m\sigma^n\eta'\eta^\dagger q^m\sigma^n\xi. \end{aligned} \quad (52)$$

We have expressed this in a form that makes it as easy as possible to match with (35), which is the term proportional to  $n_f\alpha_s^3$  on the QCD side of the matching condition. In particular, we have expanded out a factor of  $(N-1)(N+2)$  to get the constant  $-\frac{7}{5}$  under the pole in  $\epsilon$ . We see that the infrared poles in  $\epsilon$  in (35) and (52) match. The remainder of that term must be matched by the term proportional to  $C_2^{(\mathbb{1},^3P)}$  in (36). The resulting expression for the coefficient is

$$C_2^{(\mathbb{1},^3P)} = \frac{8\pi}{45}\alpha_s^2(\mu)\left[1 + \left(-\frac{16}{9}\ln\frac{\mu}{2m_c} - \frac{49}{27}\right)\frac{\alpha_s}{\pi}\right]. \quad (53)$$

Shifting the renormalization scale of the QCD coupling constant to  $\mu = 2m_c$  we obtain our final result:

$$C_2^{(\underline{1},^3P)}(\mu) = \frac{8\pi}{45}\alpha_s^2(2m_c) \left[ 1 + \left( -\frac{10}{9} \ln \frac{\mu}{2m_c} - \frac{49}{27} \right) \frac{\alpha_s}{\pi} \right]. \quad (54)$$

The remaining logarithms of  $\mu$  represent the dependence of the matrix element on the renormalization scale  $\mu$  of NRQCD.

#### IV. ANNIHILATION DECAY RATES

The factorization formula (1) for the annihilation decay rate of a quarkonium state  $H$ , including all terms whose coefficients have been computed explicitly in Section III, is

$$\begin{aligned} \Gamma(H) = \frac{1}{2M_H} & \left( \frac{C^{(\underline{1},^1S)}}{m_c^2} \langle H | \psi^\dagger \chi \chi^\dagger \psi | H \rangle + \frac{C^{(\underline{8},^3S)}}{m_c^2} \langle H | \psi^\dagger \boldsymbol{\sigma} T^a \chi \cdot \chi^\dagger \boldsymbol{\sigma} T^a \psi | H \rangle^{(\mu)} \right. \\ & + \frac{C_1^{(\underline{1},^3P)}}{m_c^4} \langle H | \psi^\dagger (-\frac{i}{2} \overleftrightarrow{\mathbf{D}} \cdot \boldsymbol{\sigma}) \chi \chi^\dagger (-\frac{i}{2} \overleftrightarrow{\mathbf{D}} \cdot \boldsymbol{\sigma}) \psi | H \rangle \\ & + \frac{C_2^{(\underline{1},^3P)}(\mu)}{m_c^4} \langle H | \psi^\dagger (-\frac{i}{2} \overleftrightarrow{\mathbf{D}})^m \sigma^n \chi \chi^\dagger (-\frac{i}{2} \overleftrightarrow{\mathbf{D}})^m \sigma^n \psi | H \rangle \\ & \left. + \frac{C_3^{(\underline{1},^3P)}}{m_c^4} \langle H | \psi^\dagger (-\frac{i}{2} \overleftrightarrow{\mathbf{D}})^m \sigma^n \chi \chi^\dagger (-\frac{i}{2} \overleftrightarrow{\mathbf{D}})^n \sigma^m \psi | H \rangle + \dots \right). \quad (55) \end{aligned}$$

We have calculated the terms proportional to  $n_f \alpha_s^2$  in  $C^{(\underline{8},^3S)}$  and the terms proportional to  $\alpha_s^2$  or  $n_f \alpha_s^3$  in the other coefficients in (55). The  $\mu$ -dependence of the coefficient  $C_2^{(\underline{1},^3P)}$  cancels that of the renormalized matrix element, which satisfies

$$\begin{aligned} \mu \frac{d}{d\mu} & \langle H | \psi^\dagger \boldsymbol{\sigma} T^a \chi \cdot \chi^\dagger \boldsymbol{\sigma} T^a \psi | H \rangle^{(\mu)} \\ & = \frac{16}{27\pi} \frac{\alpha_s(\mu)}{m_c^2} \langle H | \psi^\dagger (-\frac{i}{2} \overleftrightarrow{\mathbf{D}})^m \sigma^n \chi \chi^\dagger (-\frac{i}{2} \overleftrightarrow{\mathbf{D}})^m \sigma^n \psi | H \rangle. \quad (56) \end{aligned}$$

The relative importance of the various terms in the annihilation decay rates (55) depends on the quarkonium state. The magnitude of a particular term is determined by the order in  $\alpha_s$  of its short-distance coefficient and by the scaling of the matrix element with  $v$ , which is given by the velocity-scaling rules of NRQCD [1]. Below, we apply this general formula to the annihilation decay rates of spin-singlet S-wave states and spin-triplet P-wave states.

### A. Spin-singlet S-wave states

The dominant Fock state of the  $\eta_c$  consists of a  $c\bar{c}$  pair in a color-singlet  $^1S_0$  state. The largest matrix element that appears in the NRQCD factorization formula for the decay rate is therefore  $\langle \eta_c | \psi^\dagger \chi \chi^\dagger \psi | \eta_c \rangle$ , which scales as  $v^3$ . The next most important matrix element is  $\langle \eta_c | (\psi^\dagger \chi \chi^\dagger \mathbf{D}^2 \psi + \text{h.c.}) | \eta_c \rangle$ , which is suppressed by a factor of  $v^2$ . Matrix elements whose dominant contributions come from higher Fock states are suppressed by  $v^3$  or more. For example, the matrix element whose dominant contribution comes from the  $c\bar{c}g$  Fock state in which the  $c\bar{c}$  pair is in a color-octet  $^1P_1$  state is suppressed by  $v^4$ , with one factor of  $v^2$  arising from the probability of the  $c\bar{c}g$  Fock state and the other arising from the derivatives in the P-wave operator. The matrix element  $\langle \eta_c | \psi^\dagger \boldsymbol{\sigma} T^a \chi \cdot \chi^\dagger \boldsymbol{\sigma} T^a \psi | \eta_c \rangle$ , whose dominant contribution comes from the  $c\bar{c}g$  Fock state in which the  $c\bar{c}$  pair is in a color-octet  $^3S_1$  state, is suppressed by  $v^3$  from the probability of that  $c\bar{c}g$  Fock state. Thus, up to corrections of relative order  $v^2$ , the annihilation decay rate can be written

$$\Gamma(\eta_c) = \frac{1}{2M_{\eta_c}} \frac{C(^1S)}{m_c^2} \langle \eta_c | \psi^\dagger \chi \chi^\dagger \psi | \eta_c \rangle. \quad (57)$$

The short-distance coefficient, including the next-to-leading order correction proportional to  $n_f \alpha_s^3$ , is given in (42). The  $n_f \alpha_s^3$  term agrees with the complete next-to-leading order correction calculated by Barbieri et al. [8] and by Hagiwara et al. [9].

The difference between the matrix element in (57) and the standard NRQCD matrix element  $\langle \eta_c | \mathcal{O}_1(^1S_0) | \eta_c \rangle$  introduced in Ref. [1] is discussed in Appendix B of [2]. Up to corrections of relative order  $v^2$ , the difference is simply an overall normalization factor:

$$\langle \eta_c | \psi^\dagger \chi \chi^\dagger \psi | \eta_c \rangle \approx 4m_c \langle \eta_c | \mathcal{O}_1(^1S_0) | \eta_c \rangle. \quad (58)$$

Using the vacuum-saturation approximation, this matrix element can be related to the radial wavefunction of the  $\eta_c$  evaluated at the origin:

$$\langle \eta_c | \mathcal{O}_1(^1S_0) | \eta_c \rangle \approx \frac{3}{2\pi} |R_{\eta_c}(0)|^2. \quad (59)$$

This approximation is accurate up to corrections of relative order  $v^4$ .

## B. Spin-triplet P-wave states

The dominant Fock state of the  $\chi_{cJ}$  consists of a  $c\bar{c}$  pair in a color-singlet  ${}^3P_J$  state. This Fock state gives the dominant contributions to the color-singlet P-wave matrix elements in (55). Since the derivatives in the P-wave operators give a suppression by  $v^2$ , the color-singlet P-wave matrix elements scale as  $v^5$ . The matrix element  $\langle \chi_{cJ} | \psi^\dagger \boldsymbol{\sigma} T^a \chi \cdot \chi^\dagger \boldsymbol{\sigma} T^a \psi | \chi_{cJ} \rangle$ , whose dominant contribution comes from the  $c\bar{c}g$  Fock state in which the  $c\bar{c}$  pair is in a color-octet  ${}^3S_1$  state, is suppressed by a factor of  $v^2$  from the probability of that  $c\bar{c}g$  Fock State. Thus, it also scales like  $v^5$ , like the color-singlet P-wave matrix elements. All other matrix elements are suppressed by  $v^2$  or more. Thus, up to corrections of relative order  $v^2$ , the decay rate is given by the sum of the color-octet S-wave term and the three color-singlet P-wave terms in the NRQCD factorization formula (55).

We will use rotational symmetry and the approximate heavy-quark spin symmetry of NRQCD to show that the color-octet S-wave matrix elements  $\langle \chi_{cJ} | \psi^\dagger \boldsymbol{\sigma} T^a \chi \cdot \chi^\dagger \boldsymbol{\sigma} T^a \psi | \chi_{cJ} \rangle$  for the three  $\chi_{cJ}$  states are equal up to corrections of relative order  $v^2$ . Spin symmetry implies that the state  $\chi_{cJ}(j_z)$ , which is an eigenstate of  $\mathbf{J}^2$  and  $J_z$ , can be expressed in the form

$$|\chi_{cJ}(j_z)\rangle \approx \sum_{l_z s_z} \langle 1l_z; 1s_z | Jj_z \rangle |\chi_c(l_z s_z)\rangle, \quad (60)$$

where  $\chi_c(l_z s_z)$  is an eigenstate of  $L_z$  and  $S_z$ . Thus the color-octet  ${}^3S_1$  matrix element can be written

$$\begin{aligned} \langle \chi_{cJ} | \psi^\dagger \boldsymbol{\sigma} T^a \chi \cdot \chi^\dagger \boldsymbol{\sigma} T^a \psi | \chi_{cJ} \rangle &\equiv \frac{1}{2J+1} \sum_{j_z} \langle \chi_{cJ}(j_z) | \psi^\dagger \boldsymbol{\sigma} T^a \chi \cdot \chi^\dagger \boldsymbol{\sigma} T^a \psi | \chi_{cJ}(j_z) \rangle \\ &\approx \frac{1}{2J+1} \sum_{j_z} \sum_{l'_z s'_z} \sum_{l_z s_z} \langle Jj_z | 1l'_z; 1s'_z \rangle \langle 1l_z; 1s_z | Jj_z \rangle \\ &\quad \times \langle \chi_c(l'_z s'_z) | \psi^\dagger \sigma^i T^a \chi \chi^\dagger \sigma^i T^a \psi | \chi_c(l_z s_z) \rangle. \end{aligned} \quad (61)$$

Spin symmetry also implies that the matrix element on the right side of (61) is proportional to  $U_{is'_z}^\dagger U_{s_z i}$ , where  $U_{mi}$  is the unitary  $3 \times 3$  matrix that transforms vectors from the Cartesian basis to the spherical basis. Finally, rotational symmetry implies that matrix elements on

the right side of (61) must be proportional to  $\delta_{l'_z l_z}$ . Using the orthogonality relations of the Clebsch-Gordan coefficients, the equation (61) can be reduced to

$$\langle \chi_{cJ} | \psi^\dagger \boldsymbol{\sigma} T^a \chi \cdot \chi^\dagger \boldsymbol{\sigma} T^a \psi | \chi_{cJ} \rangle \approx \langle \chi_{c0} | \psi^\dagger \boldsymbol{\sigma} T^a \chi \cdot \chi^\dagger \boldsymbol{\sigma} T^a \psi | \chi_{c0} \rangle. \quad (62)$$

These relations hold up to corrections of relative order  $v^2$ .

We next show that the color-singlet P-wave matrix elements in (55) can be reduced to a single independent matrix element, which we choose to be  $\langle \chi_{c0} | \psi^\dagger (-\frac{i}{2} \overleftrightarrow{\mathbf{D}} \cdot \boldsymbol{\sigma}) \chi \chi^\dagger (-\frac{i}{2} \overleftrightarrow{\mathbf{D}} \cdot \boldsymbol{\sigma}) \psi | \chi_{c0} \rangle$ . Using the expression (60) for the  $\chi_{cJ}$  states, we can write

$$\begin{aligned} \langle \chi_{cJ} | \psi^\dagger (-\frac{i}{2} \overleftrightarrow{\mathbf{D}})^m \sigma^n \chi \chi^\dagger (-\frac{i}{2} \overleftrightarrow{\mathbf{D}})^i \sigma^j \psi | \chi_{cJ} \rangle &\approx \frac{1}{2J+1} \sum_{j_z} \sum_{l'_z s'_z} \sum_{l_z s_z} \langle J j_z | 1 l'_z; 1 s'_z \rangle \langle 1 l_z; 1 s_z | J j_z \rangle \\ &\times \langle \chi_c(l'_z s'_z) | \psi^\dagger (-\frac{i}{2} \overleftrightarrow{\mathbf{D}})^m \sigma^n \chi \chi^\dagger (-\frac{i}{2} \overleftrightarrow{\mathbf{D}})^i \sigma^j \psi | \chi_c(l_z s_z) \rangle. \end{aligned} \quad (63)$$

The vacuum-saturation approximation, which is accurate up to corrections of relative order  $v^4$  can be used to express the matrix element on the right side of (63) as the product of  $\langle \chi_c(l'_z s'_z) | \chi^\dagger (-\frac{i}{2} \overleftrightarrow{\mathbf{D}})^m \sigma^n \psi | 0 \rangle$  and  $\langle 0 | \psi^\dagger (-\frac{i}{2} \overleftrightarrow{\mathbf{D}})^i \sigma^j \chi | \chi_c(l_z s_z) \rangle$ . Rotational symmetry and spin symmetry imply that these two matrix elements are proportional to  $U_{m l'_z}^\dagger U_{n s'_z}^\dagger$  and  $U_{l_z i} U_{s_z j}$ , respectively. Thus the tensorial structure of the matrix element (63) is completely determined. The proportionality constant can be deduced by taking the special case  $J = 0$ ,  $i = j$  and  $m = n$ , summed over  $i$  and  $m$ . The resulting formula is

$$\begin{aligned} \langle \chi_{cJ} | \psi^\dagger (-\frac{i}{2} \overleftrightarrow{\mathbf{D}})^i \sigma^j \chi \chi^\dagger (-\frac{i}{2} \overleftrightarrow{\mathbf{D}})^m \sigma^n \psi | \chi_{cJ} \rangle &\approx \frac{1}{3} \langle \chi_{c0} | \psi^\dagger (-\frac{i}{2} \overleftrightarrow{\mathbf{D}} \cdot \boldsymbol{\sigma}) \chi \chi^\dagger (-\frac{i}{2} \overleftrightarrow{\mathbf{D}} \cdot \boldsymbol{\sigma}) \psi | \chi_{c0} \rangle \\ &\times \frac{1}{2J+1} \sum_{j_z} \sum_{l'_z s'_z} \sum_{l_z s_z} \langle J j_z | 1 l'_z; 1 s'_z \rangle \langle 1 l_z; 1 s_z | J j_z \rangle U_{m l'_z}^\dagger U_{n s'_z}^\dagger U_{l_z i} U_{s_z j}. \end{aligned} \quad (64)$$

The scalar combinations of these matrix elements can be simplified by using the identity  $(UU^t)_{m_1 m_2} = -\sqrt{3} \langle 1 m_1; 1 m_2 | 00 \rangle$  together with the orthogonality relations for Clebsch-Gordan coefficients. The resulting formulas are

$$\begin{aligned} \langle \chi_{cJ} | \psi^\dagger (-\frac{i}{2} \overleftrightarrow{\mathbf{D}} \cdot \boldsymbol{\sigma}) \chi \chi^\dagger (-\frac{i}{2} \overleftrightarrow{\mathbf{D}} \cdot \boldsymbol{\sigma}) \psi | \chi_{cJ} \rangle \\ \approx \delta_{J0} \langle \chi_{c0} | \psi^\dagger (-\frac{i}{2} \overleftrightarrow{\mathbf{D}} \cdot \boldsymbol{\sigma}) \chi \chi^\dagger (-\frac{i}{2} \overleftrightarrow{\mathbf{D}} \cdot \boldsymbol{\sigma}) \psi | \chi_{c0} \rangle, \end{aligned} \quad (65a)$$

$$\langle \chi_{cJ} | \psi^\dagger (-\frac{i}{2} \overleftrightarrow{\mathbf{D}})^m \sigma^n \chi \chi^\dagger (-\frac{i}{2} \overleftrightarrow{\mathbf{D}})^m \sigma^n \psi | \chi_{cJ} \rangle$$

$$\approx \frac{1}{3} \langle \chi_{c0} | \psi^\dagger (-\frac{i}{2} \overleftrightarrow{\mathbf{D}} \cdot \boldsymbol{\sigma}) \chi \chi^\dagger (-\frac{i}{2} \overleftrightarrow{\mathbf{D}} \cdot \boldsymbol{\sigma}) \psi | \chi_{c0} \rangle, \quad (65b)$$

$$\begin{aligned} & \langle \chi_{cJ} | \psi^\dagger (-\frac{i}{2} \overleftrightarrow{\mathbf{D}})^m \sigma^n \chi \chi^\dagger (-\frac{i}{2} \overleftrightarrow{\mathbf{D}})^n \sigma^m \psi | \chi_{cJ} \rangle \\ & \approx (-1)^J \frac{1}{3} \langle \chi_{c0} | \psi^\dagger (-\frac{i}{2} \overleftrightarrow{\mathbf{D}} \cdot \boldsymbol{\sigma}) \chi \chi^\dagger (-\frac{i}{2} \overleftrightarrow{\mathbf{D}} \cdot \boldsymbol{\sigma}) \psi | \chi_{c0} \rangle. \end{aligned} \quad (65c)$$

Using the relations (62) and (65), the dominant terms in the decay rates for the  $\chi_{cJ}$  reduce to

$$\begin{aligned} \Gamma(\chi_{cJ}) = \frac{1}{2M_{\chi_{cJ}}} & \left( \frac{C^{(\underline{\mathbf{3}},^3S)} }{m_c^2} \langle \chi_{c0} | \psi^\dagger \boldsymbol{\sigma} T^a \chi \cdot \chi^\dagger \boldsymbol{\sigma} T^a \psi | \chi_{c0} \rangle^{(\mu)} \right. \\ & \left. + \frac{C^{(\underline{\mathbf{1}},^3P_J)}(\mu)}{m_c^4} \langle \chi_{c0} | \psi^\dagger (-\frac{i}{2} \overleftrightarrow{\mathbf{D}} \cdot \boldsymbol{\sigma}) \chi \chi^\dagger (-\frac{i}{2} \overleftrightarrow{\mathbf{D}} \cdot \boldsymbol{\sigma}) \psi | \chi_{c0} \rangle \right), \end{aligned} \quad (66)$$

where  $C^{(\underline{\mathbf{1}},^3P_J)}$  is a linear combination of the coefficients  $C_n^{(\underline{\mathbf{1}},^3P)}$ ,  $n = 1, 2, 3$ :

$$C^{(\underline{\mathbf{1}},^3P_J)}(\mu) = \delta_{J0} C_1^{(\underline{\mathbf{1}},^3P)} + \frac{1}{3} C_2^{(\underline{\mathbf{1}},^3P)}(\mu) + \frac{(-1)^J}{3} C_3^{(\underline{\mathbf{1}},^3P)}. \quad (67)$$

In explicit form, these coefficients are

$$C^{(\underline{\mathbf{1}},^3P_0)}(\mu) = \frac{4\pi}{9} \alpha_s^2 (2m_c) \left[ 1 - \frac{4}{27} \left( \ln \frac{\mu}{2m_c} + \frac{29}{6} \right) n_f \frac{\alpha_s}{\pi} \right], \quad (68a)$$

$$C^{(\underline{\mathbf{1}},^3P_1)}(\mu) = \frac{4\pi}{9} \alpha_s^2 (2m_c) \left[ 0 - \frac{4}{27} \left( \ln \frac{\mu}{2m_c} + \frac{4}{3} \right) n_f \frac{\alpha_s}{\pi} \right], \quad (68b)$$

$$C^{(\underline{\mathbf{1}},^3P_2)}(\mu) = \frac{4\pi}{9} \alpha_s^2 (2m_c) \left[ \frac{4}{15} - \frac{4}{27} \left( \ln \frac{\mu}{2m_c} + \frac{29}{15} \right) n_f \frac{\alpha_s}{\pi} \right]. \quad (68c)$$

The constants  $Q_J$  under the logarithm in these three expressions are

$$Q_0 = \frac{29}{6}, \quad Q_1 = \frac{4}{3}, \quad Q_2 = \frac{29}{15}. \quad (69)$$

Up to corrections of relative order  $v^2$ , the matrix elements in (66) are related to the standard matrix elements defined in Ref. [1] by a simple normalization factor:

$$\langle \chi_{c0} | \psi^\dagger \boldsymbol{\sigma} T^a \chi \cdot \chi^\dagger \boldsymbol{\sigma} T^a \psi | \chi_{c0} \rangle \approx 4m_c \langle \chi_{c0} | \mathcal{O}_8(^3S_1) | \chi_{c0} \rangle, \quad (70)$$

$$\langle \chi_{c0} | \psi^\dagger (-\frac{i}{2} \overleftrightarrow{\mathbf{D}} \cdot \boldsymbol{\sigma}) \chi \chi^\dagger (-\frac{i}{2} \overleftrightarrow{\mathbf{D}} \cdot \boldsymbol{\sigma}) \psi | \chi_{c0} \rangle \approx 12m_c \langle \chi_{c0} | \mathcal{O}_1(^3P_0) | \chi_{c0} \rangle. \quad (71)$$

Using the vacuum-saturation approximation, the matrix element  $\langle \chi_{c0} | \mathcal{O}_1(^3P_0) | \chi_{c0} \rangle$  can be expressed in terms of the derivative of the radial wavefunction for the  $\chi_{c0}$  evaluated at the origin:

$$\langle \chi_{c0} | \mathcal{O}_1(^3P_0) | \chi_{c0} \rangle \approx \frac{27}{2\pi} |R'_{\chi_{c0}}(0)|^2. \quad (72)$$

The corrections are of relative order  $v^4$ .

We now compare our results for  $C(^{\underline{1}}^3P_J)$  with previous calculations of these coefficients to order  $\alpha_s^3$ . Our results agree with the  $n_f \alpha_s^3$  terms obtained in recent calculations by Huang and Chao [6] and by Petrelli [7], who also used dimensional regularization as the infrared cutoff for divergences associated with the emission of a soft gluon. Our coefficients need not agree with those in the original calculations by Barbieri et al. [4,5], since they used different infrared cutoffs. However any differences in  $C(^{\underline{1}}^3P_J)$  must be compensated by differences in the matrix element  $\langle \chi_{c0} | \psi^\dagger \boldsymbol{\sigma} T^a \chi \cdot \chi^\dagger \boldsymbol{\sigma} T^a \psi | \chi_{c0} \rangle$  in the factorization formula (66). This implies that the differences between the coefficients  $C(^{\underline{1}}^3P_J)$  obtained with two different infrared cutoffs must be independent of  $J$ .

In Ref. [4], Barbieri et al. calculated the coefficients of the color-singlet matrix element in the decay rates of the  $\chi_{c0}$  and  $\chi_{c2}$  using the binding energy of the  $c\bar{c}$  pair to regularize the infrared divergences that arise from the emission of a soft gluon. Taking the annihilating  $c\bar{c}$  pair to have invariant mass  $M$ , the infrared divergence shows up as a logarithm of  $M^2 - 4m_c^2$ . This cutoff can be translated into an equivalent cutoff  $\Lambda$  on the momentum of the soft gluon by replacing  $\ln(4m_c^2/(M^2 - 4m_c^2)) \rightarrow -\ln(\Lambda/m_c)$ . In Ref. [5], Barbieri et al. calculated the decay rates of  $\chi_{c0}$ ,  $\chi_{c1}$ , and  $\chi_{c2}$  into two-jet configurations defined by an angular resolution  $\delta$  and a fractional energy resolution  $\epsilon$ . Their result for  $\chi_{c1}$  is independent of  $\delta$  and depends logarithmically on  $\epsilon$ . This cutoff can be translated into an equivalent infrared cutoff  $\Lambda$  on the momentum of the soft gluon by replacing  $\ln(2\epsilon) \rightarrow \ln(\Lambda/m_c)$ . Expressing the results of Barbieri et al. in the same form as in (68), the expressions inside the parentheses are  $\ln(\Lambda/m_c) + Q'_J$ , where the numbers  $Q'_J$  are

$$Q'_0 = 4, \quad Q'_1 = \frac{1}{2}, \quad Q'_2 = \frac{11}{10}. \quad (73)$$

Comparing the coefficients in (69) and (73), we see that  $Q_J - Q'_J = \frac{5}{6}$ , independent of  $J$ . Thus the differences between the two calculations correspond simply to different choices for



the definition of the color-octet matrix element. The relation between the matrix elements in the two calculations is

$$\begin{aligned} \langle \chi_{c0} | \psi^\dagger \boldsymbol{\sigma} T^a \chi \cdot \chi^\dagger \boldsymbol{\sigma} T^a \psi | \chi_{c0} \rangle^{(\mu)} \Big|_{\text{dim.reg.}} &= \langle \chi_{c0} | \psi^\dagger \boldsymbol{\sigma} T^a \chi \cdot \chi^\dagger \boldsymbol{\sigma} T^a \psi | \chi_{c0} \rangle^{(\Lambda)} \Big|_{\text{cutoff}} \\ &+ \frac{16\alpha_s}{81\pi m_c^2} \left( \ln \frac{\mu}{2\Lambda} + \frac{5}{6} \right) \langle \chi_{c0} | \psi^\dagger (-\frac{i}{2} \overleftrightarrow{\mathbf{D}} \cdot \boldsymbol{\sigma}) \chi \chi^\dagger (-\frac{i}{2} \overleftrightarrow{\mathbf{D}} \cdot \boldsymbol{\sigma}) \psi | \chi_{c0} \rangle. \end{aligned} \quad (74)$$

This identification can be verified by repeating the calculation of the coefficient  $C_2^{(1,3P)}$  in Section III using an infrared momentum cutoff  $\Lambda$ . On the QCD side of the matching condition, one must put a cutoff  $x > \Lambda/m_c$  on the integral in (26) for  $n = 0$ . On the NRQCD side, one must put a cutoff  $k > \Lambda$  on the integral in (47). The relation (74) is identical to the relation between the corresponding production matrix elements defined by dimensional regularization and by a momentum cutoff, which was found in Ref. [3].

In Ref. [10] and [11], Mangano and Petrelli used the next-to-leading order results of Barbieri et al. for  $\chi_{c0}$  and  $\chi_{c2}$ , but they performed an independent calculation for  $\chi_{c1}$ . Their result corresponds to  $Q'_1 = -\frac{7}{3}$ . Since this result disagrees with four other independent calculations, we conclude that it is incorrect.

## V. CONCLUSIONS

In the NRQCD factorization framework, the short-distance coefficients in annihilation decay rates and in inclusive production cross sections can be calculated systematically as a power series in  $\alpha_s(m_c)$ . For most applications, next-to-leading order calculations are essential for accurate predictions. Dimensional regularization is the most convenient method for regularizing the infrared and ultraviolet divergences that arise in calculations beyond leading order in  $\alpha_s$ . The generalization of the threshold expansion method to  $N$  dimensions allows dimensional regularization to be used consistently in quarkonium calculations. In this paper, we used this method to calculate the terms proportional to  $n_f \alpha_s^3$  in the short-distance coefficients of color-singlet matrix elements in the annihilation decay rates of P-wave charmonium states, thus resolving the discrepancies between previous calculations. Our results agree with

the original calculations by Barbieri et al. after allowing for differences in the color-octet matrix element due to different infrared cutoffs. Our results also agree with recent calculations using covariant projection methods in conjunction with dimensional regularization. In conclusion, the threshold expansion method combined with dimensional regularization provides a general and powerful method for carrying out quarkonium calculations beyond leading order in  $\alpha_s$ .

### ACKNOWLEDGMENTS

This work was supported in part by the U.S. Department of Energy, Division of High Energy Physics, under Grant DE-FG02-91-ER40684.

### APPENDIX A: NONRELATIVISTIC EXPANSION OF SPINORS

In this Appendix, we present the formulas for the nonrelativistic approximations of spinors that are needed to calculate short-distance coefficients for heavy quarkonium decay rates using the threshold expansion method. All the formulas below hold in  $N$  spatial dimensions. The representation for gamma matrices that is most convenient for carrying out the nonrelativistic expansion of a spinor is the Dirac representation:

$$\gamma^0 = \begin{pmatrix} 1 & 0 \\ 0 & -1 \end{pmatrix}, \quad \gamma^i = \begin{pmatrix} 0 & \sigma^i \\ -\sigma^i & 0 \end{pmatrix}. \quad (\text{A1})$$

In the center-of-momentum (CM) frame of the  $c\bar{c}$  pair, their momenta  $p$  and  $\bar{p}$  of the  $c$  and  $\bar{c}$  can be written

$$p = (E_q, \mathbf{q}), \quad (\text{A2a})$$

$$\bar{p} = (E_q, -\mathbf{q}), \quad (\text{A2b})$$

where  $E_q = \sqrt{m_c^2 + \mathbf{q}^2}$ . The spinors for the  $c$  and the  $\bar{c}$  in the CM frame are

$$u(p) = \frac{1}{\sqrt{E_q + m_c}} \begin{pmatrix} (E_q + m_c) \xi \\ \mathbf{q} \cdot \boldsymbol{\sigma} \xi \end{pmatrix}, \quad (\text{A3a})$$

$$v(\bar{p}) = \frac{1}{\sqrt{E_q + m_c}} \begin{pmatrix} -\mathbf{q} \cdot \boldsymbol{\sigma} \eta \\ (E_q + m_c) \eta \end{pmatrix}. \quad (\text{A3b})$$

Color and spin quantum numbers on the Dirac spinors and on the Pauli spinors  $\eta$  and  $\xi$  are suppressed. If the Pauli spinors are normalized so that  $\eta^\dagger \eta = \xi^\dagger \xi = 1$ , the spinors in (A3) satisfy  $\bar{u}u = -\bar{v}v = 2m_c$ .

The independent quantities that can be formed by sandwiching 3 or fewer Dirac matrices between  $\bar{v}(\bar{p})$  and  $u(p)$  are

$$\bar{v}(\bar{p})u(p) = -2 \eta^\dagger(\mathbf{q} \cdot \boldsymbol{\sigma})\xi, \quad (\text{A4a})$$

$$\bar{v}(\bar{p})\gamma^\mu u(p) = -g^{\mu j} \left( 2E_q \eta^\dagger \sigma^j \xi - \frac{2}{E_q + m_c} q^j \eta^\dagger(\mathbf{q} \cdot \boldsymbol{\sigma})\xi \right), \quad (\text{A4b})$$

$$\begin{aligned} \bar{v}(\bar{p})(\gamma^\mu \gamma^\nu - \gamma^\nu \gamma^\mu)u(p) &= 4(g^{\mu 0} g^{\nu j} - g^{\nu 0} g^{\mu j}) \left( m_c \eta^\dagger \sigma^j \xi + \frac{1}{E_q + m_c} q^j \eta^\dagger(\mathbf{q} \cdot \boldsymbol{\sigma})\xi \right) \\ &\quad + g^{\mu j} g^{\nu k} \eta^\dagger \{[\sigma^j, \sigma^k], \mathbf{q} \cdot \boldsymbol{\sigma}\} \xi, \end{aligned} \quad (\text{A4c})$$

$$\begin{aligned} \bar{v}(\bar{p})(\gamma^\mu \gamma^\nu \gamma^\mu - \gamma^\mu \gamma^\nu \gamma^\mu)u(p) &= g^{\mu i} g^{\nu j} g^{\mu k} \left( E_q \eta^\dagger \{[\sigma^i, \sigma^j], \sigma^k\} \xi - \frac{q^i}{E_q + m_c} \eta^\dagger \{[\sigma^j, \sigma^k], \mathbf{q} \cdot \boldsymbol{\sigma}\} \xi \right. \\ &\quad \left. - \frac{q^j}{E_q + m_c} \eta^\dagger \{[\sigma^k, \sigma^i], \mathbf{q} \cdot \boldsymbol{\sigma}\} \xi - \frac{q^k}{E_q + m_c} \eta^\dagger \{[\sigma^i, \sigma^j], \mathbf{q} \cdot \boldsymbol{\sigma}\} \xi \right) \\ &\quad + 4 \left( g^{\mu 0} g^{\nu i} g^{\mu j} + g^{\nu 0} g^{\mu i} g^{\mu j} + g^{\mu 0} g^{\mu i} g^{\nu j} \right) \left( \eta^\dagger q^i \sigma^j \xi - \eta^\dagger q^j \sigma^i \xi \right). \end{aligned} \quad (\text{A4d})$$

These expressions can be obtained from the corresponding spinor factors in Appendix A of Ref. [3] by setting  $L_j^\mu = -g^{\mu j} = \delta^{\mu j}$  and  $P^\mu = 2E_q g^{\mu 0}$  and by taking the hermitian conjugate. Using the expressions for the spinor factors in (A4), it is easy to carry out their nonrelativistic expansions in powers of  $\mathbf{q}$ .

## REFERENCES

- [1] G.T. Bodwin, E. Braaten, and G.P. Lepage, Phys. Rev. **D51**, 1125 (1995).
- [2] E. Braaten and Y.-Q. Chen, Phys. Rev. **D54**, 3216 (1996).
- [3] E. Braaten and Y.-Q. Chen, OHSTPY-HEP-T-96-018 (hep-ph/9610401), to appear in Phys. Rev. D.
- [4] R. Barbieri, M. Gaffo, R. Gatto and E. Remiddi, Nucl. Phys. **B192**, 61 (1981).
- [5] R. Barbieri, M. Caffo, and E. Remiddi, Nucl. Phys. **B162**, 220 (1980).
- [6] H.-W. Huang and K.-T. Chao, Phys. Rev. **D54** 6850 (1996). (An error in the published paper is corrected in hep-ph/9606220 v3.)
- [7] A. Petrelli, Ph.D. thesis, University of Pisa, Italy, December 1996 (private communication).
- [8] R. Barbieri, G. Curci, E. d'Emilio, and E. Remiddi, Nucl. Phys. **B154**, 535 (1979).
- [9] K. Hagiwara, C.B. Kim, and T. Yoshino, Nucl. Phys. **B177**, 461 (1981).
- [10] M.L. Mangano and A. Petrelli, Phys. Lett. **B352**, 445 (1995).
- [11] A. Petrelli, Phys. Lett. **B380**, 159 (1996).

## FIGURES

Fig. 1. The lowest-order cut Feynman diagram in QCD that are associated with the process  $c\bar{c} \rightarrow q\bar{q}$ .

Fig. 2. The lowest-order cut Feynman diagrams in QCD that are associated with the process  $c\bar{c} \rightarrow q\bar{q}g$ .

Fig. 3. The lowest-order cut Feynman diagrams in QCD that are associated with the process  $c\bar{c} \rightarrow gg$ .

Fig. 4. The lowest-order Feynman diagram for NRQCD matrix elements such as  $\langle c\bar{c}' | \psi^\dagger \boldsymbol{\sigma} T^a \chi \cdot \chi^\dagger \boldsymbol{\sigma} T^a \psi | c\bar{c} \rangle$ .

Fig. 5. The next-to-leading-order Feynman diagrams for the NRQCD matrix element  $\langle c\bar{c}' | \psi^\dagger \boldsymbol{\sigma} T^a \chi \cdot \chi^\dagger \boldsymbol{\sigma} T^a \psi | c\bar{c} \rangle$  when the initial and final  $c\bar{c}$  pairs are in color-singlet states.

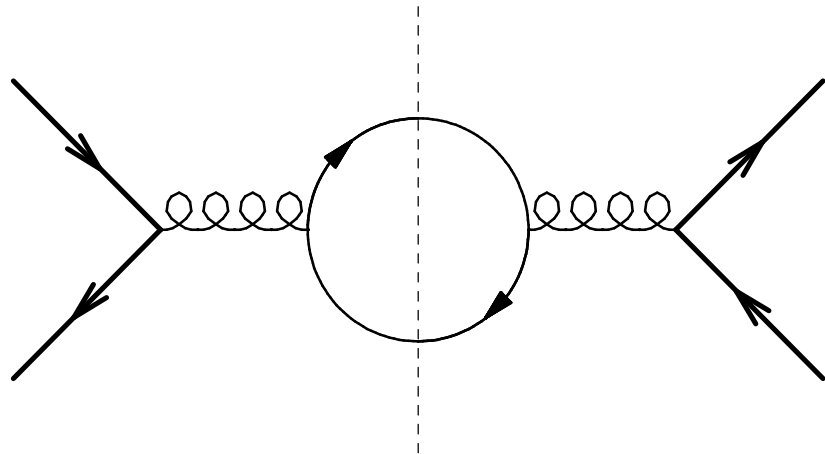


Figure 1

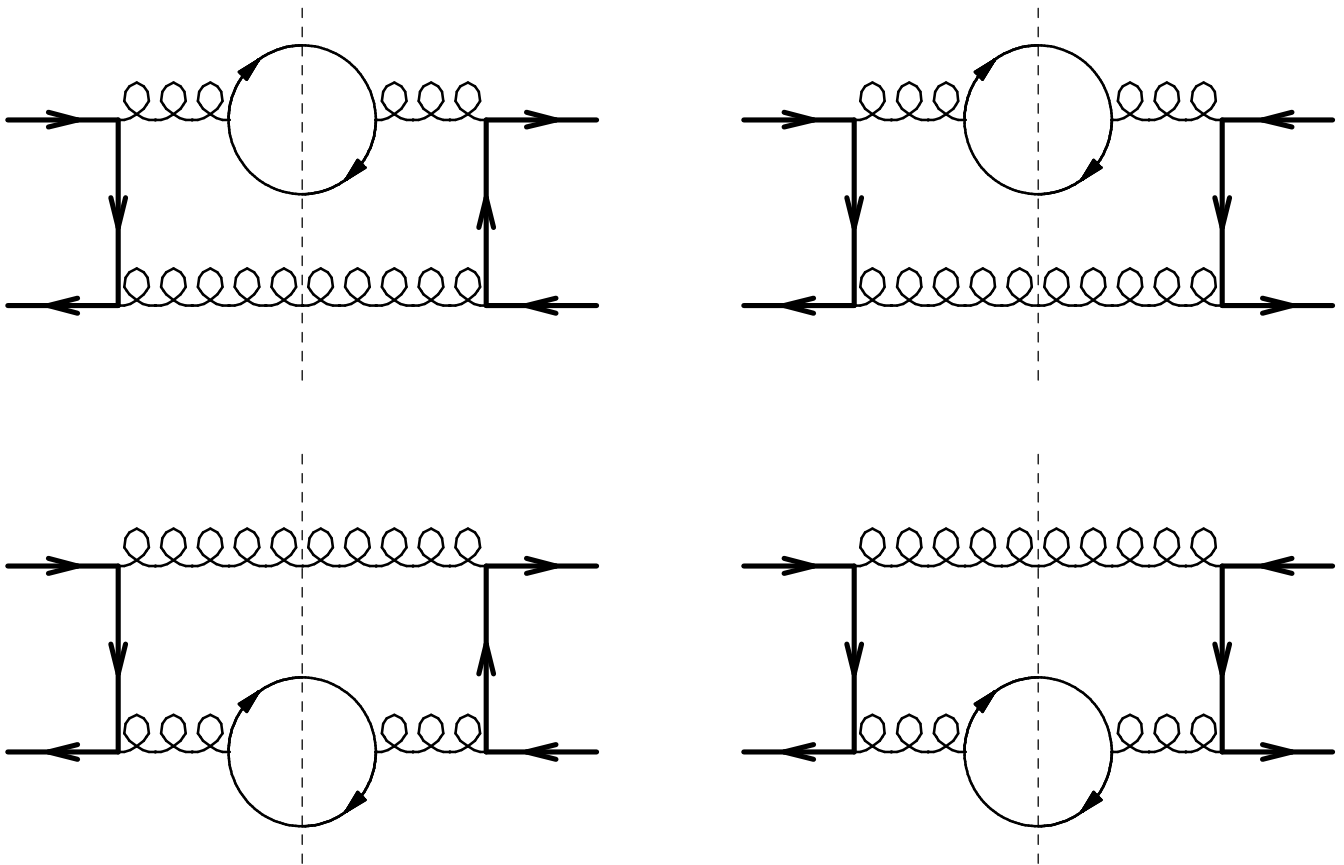


Figure 2

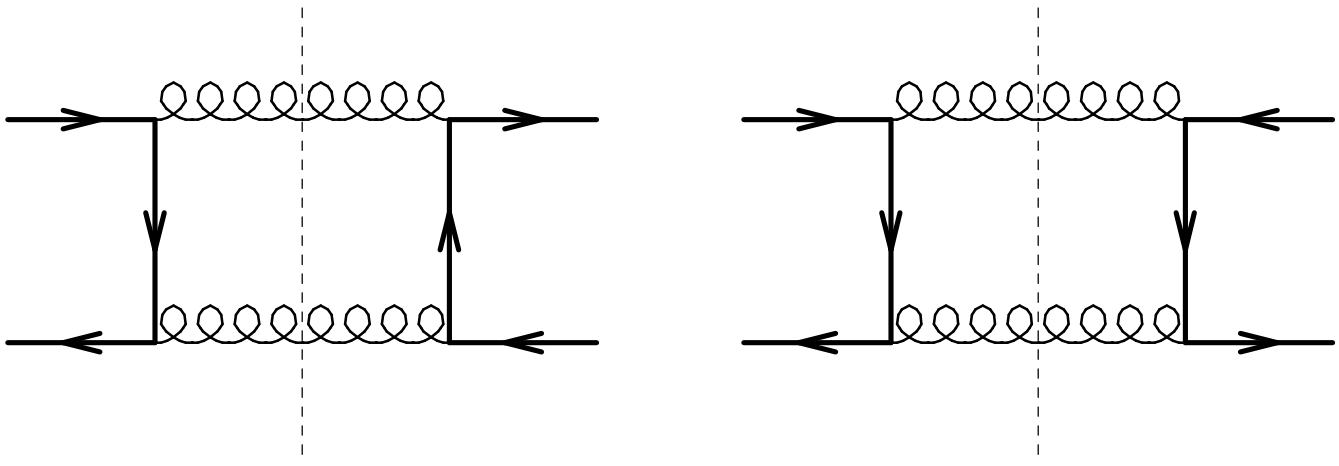


Figure 3

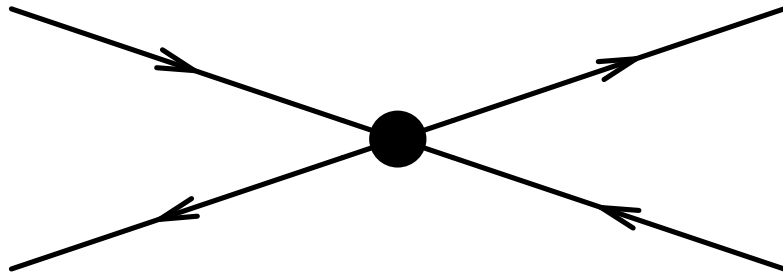


Figure 4

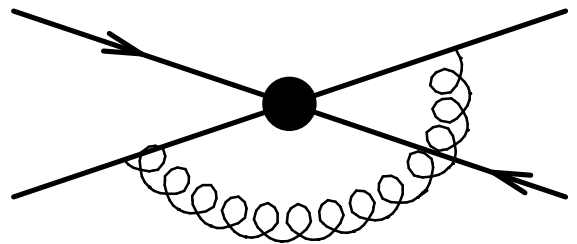
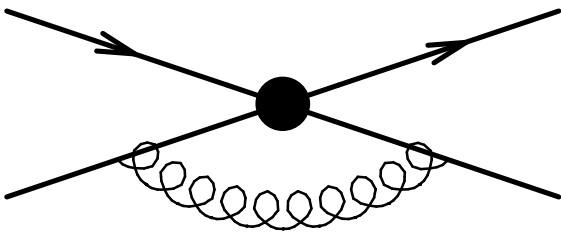
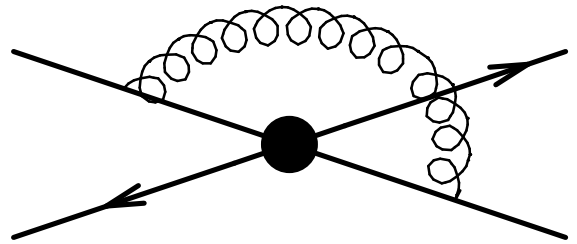
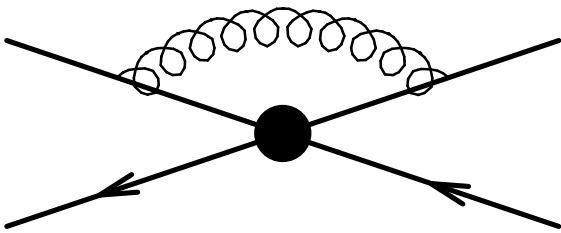


Figure 5